EXPERIMENTAL STUDY OF BRIDGE ELASTOMER AND OTHER ISOLATION AND ENERGY DISSIPATION SYSTEMS WITH EMPHASIS ON UPLIFT PREVENTION AND HIGH VELOCITY NEAR-SOURCE SEISMIC EXCITATION

by

Amarnath Kasalanati

and

Michael C. Constantinou

July 1998

SECTION 6 IS AN EXCERPT FROM THE DOCTORAL DISSERTATION BY THE FIRST AUTHOR. THIS SECTION OF THE REPORT HAS BEEN EXTRACTED SINCE IT APPLIES TO THE USE OF FLUID VISCOUS DAMPERS.

THE ENTIRE REPORT CAN BE REVIEWED AT THE STATE UNIVERSITY OF NEW YORK AT BUFFALO, SCIENCE AND ENGINEERING LIBRARY, LOCATED IN THE NORTH CAMPUS.

SECTION 6

RESULTS OF EARTHQUAKE SIMULATOR TESTING OF ISOLATED BRIDGE CONFIGURATIONS

6.1 Introduction

The isolated bridge configurations included low and high damping elastomeric isolation systems, and the low damping elastomeric systems with added linear and nonlinear viscous dampers. Each of these configurations could withstand much stronger seismic excitations than the non-isolated configurations. However, a set of low intensity tests was conducted to form a basis for comparison with the non-isolated configurations and also to test the effectiveness of these systems under low intensity excitation. The results of these tests are presented in this section, followed by an interpretation which focuses on the effects of scragging, the benefits of seismic isolation, the significance of damping, the importance of added damping in near-source seismic excitation, and on the benefits and drawbacks of using nonlinear viscous damping.

6.2 Test Results

A total of 135 tests were performed on the four isolated bridge configurations. Table 6-1 presents peak values of response quantities obtained in the testing. Moreover, Appendices C to F present the results in graphical form for a number of the conducted tests. For a complete graphical presentation of the results see Kasalanati (1998). The response quantities presented in Table 6-1 are:

(a) The peak values of displacement, velocity and acceleration of the shake table. Of these, the displacement and acceleration were directly measured, whereas the velocity was obtained by numerical differentiation of the displacement record.

(b) The bearing displacement, bearing shear force, longitudinal component of damping force, and total shear force at the abutment location. These forces represent the peak values of forces on two abutments.

(c) Abutment drift measured as the displacement of the abutment top (at the connection to the load cell above) with respect to the shake table.

(d) Abutment acceleration measured at the abutment top.

(e) The bearing displacement at the flexible pier location.

(f) The pier shear force as measured by the strain gage load cells in the columns of the flexible pier.

(g) Pier drift and pier acceleration.

(h) Total shear at the isolation system level. This is the combined force in the abutment and the flexible pier bearings and the longitudinal component of the damping forces.

(i) Deck acceleration as the average of measurements by instruments AHDNE and AHDNW (instruments 5 and 6 in Figure 4-17).

The results in Table 6-1 are presented in groups corresponding to the same earthquake excitation but of varying intensity. That is, the results of tests are not presented in the sequence in which the tests were conducted. For the high damping elastomeric isolation system the sequence of testing was important since the bearings were installed without any prior testing (unscragged conditions). Special note will be made on the behavior of the system in repetitive testing when the results are interpreted.

Table 6-1: Results of Testing of Isolated Bridge Configurations

TEST	EXCITATION	PEAK TABLE MOTION			ABUTMENT						PIER				Isolation System Total Shear /Wt	DECK ACCL. (g)
		DISPL (mm)	VEL (mm/s)	ACCL. (g)	Bearing Displ. (mm)	Bearing Shear /Wt	Damper Force /Wt	Total Shear /Wt	Abut. Drift (mm)	Abut. Accl. (g)	Bearing Displ. (mm)	Pier Shear /Wt	Pier Drift (mm)	Pier Accl. (g)		
L0FS002.1	EL CENTRO S00E 100%	24.4	161.	0.35	26.1	0.072	-	0.072	0.7	0.35	21.8	0.070	3.6	0.49	0.136	0.15
L0FS003.1	EL CENTRO S00E 200%	48.7	325.	0.64	60.8	0.136	-	0.136	1.6	0.63	51.9	0.135	7.5	0.96	0.263	0.29
LLFS001.1	EL CENTRO S00E 100%	24.3	159.	0.34	11.9	0.040	0.090	0.097	0.7	0.37	10.2	0.039	2.3	0.43	0.122	0.13
LLFS002.1	EL CENTRO S00E200% - 1	48.7	313.	0.61	28.8	0.077	0.157	0.175	1.3	0.63	25.2	0.073	4.4	0.78	0.214	0.23
LLFS002.2	EL CENTRO S00E 200% - 2	53.1	349.	0.68	32.1	0.084	0.169	0.187	1.5	0.70	28.2	0.077	4.8	0.90	0.232	0.25
LNFS002.1	EL CENTRO S00E 100%	28.1	163.	0.32	8.1	0.034	0.176	0.189	2.2	0.46	6.8	0.034	2.2	0.47	0.207	0.23
LNFS003.1	EL CENTRO S00E 200%	55.9	329.	0.62	19.7	0.066	0.218	0.250	3.1	0.95	17.1	0.066	4.2	1.07	0.296	0.32
H0FS001.1	EL CENTRO S00E 200% - 1	55.7	325.	0.58	51.4	0.168	-	0.168	1.3	0.66	44.8	0.134	7.8	1.05	0.284	0.30
H0FS001.2	EL CENTRO S00E 200% - 2	55.8	328.	0.57	56.6	0.153	-	0.153	1.2	0.68	49.3	0.132	8.0	1.08	0.270	0.30
H0FS001.3	EL CENTRO S00E 200% - 3	55.6	332.	0.58	57.5	0.151	-	0.151	1.2	0.70	50.4	0.128	8.5	1.12	0.264	0.29
H0FS001.4	EL CENTRO S00E 200% - 4	55.7	333.	0.58	58.6	0.125	-	0.125	1.0	0.72	52.4	0.109	6.6	1.13	0.220	0.24
H0FS001.5	EL CENTRO S00E 200% - 5	56.0	327.	0.57	59.3	0.122	-	0.122	0.9	0.72	54.2	0.108	6.5	1.12	0.212	0.23
H0FS012.1	EL CENTRO S00E 100%	27.9	170.	0.29	25.8	0.073	-	0.073	0.5	0.35	22.8	0.065	3.7	0.51	0.131	0.14
L0FS004.1	EL CENTRO S00E H+V 100%	23.6	156.	0.30	32.4	0.084	-	0.084	0.9	0.38	27.3	0.085	4.4	0.51	0.159	0.18
L0FS005.1	EL CENTRO S00E H+V 200%	47.4	315.	0.66	71.6	0.160	-	0.160	1.7	0.78	61.2	0.159	8.7	1.20	0.306	0.34
LLFS003.1	EL CENTRO S00E H+V 100%	35.2	173.	0.35	17.0	0.053	0.094	0.102	1.3	0.42	14.9	0.051	2.8	0.51	0.144	0.16
LLFS004.1	EL CENTRO S00E H+V 200%	70.0	367.	0.70	39.8	0.102	0.170	0.194	2.5	0.70	34.8	0.093	5.5	1.21	0.274	0.31
LLFS004.2	EL CENTRO S00E H+V 200%	53.1	348.	0.68	31.8	0.085	0.172	0.192	2.9	0.69	28.3	0.078	4.9	0.91	0.229	0.26
LNFS004.1	EL CENTRO S00E H+V 100%	28.1	172.	0.33	8.2	0.033	0.177	0.189	2.2	0.47	6.9	0.034	2.1	0.46	0.208	0.23

Wt = Weight of the Deck = 140 kN
All Configurations are for Flexible North Pier and Stiff South Abutment
The Reported Forces at the Abutment Represent the Forces on Two Abutments
Bearing Displacements and Pier Drifts are Average Values from Two Measurements

L0FS - Low Damping Elastomeric Bearings (No Dampers)
LLFS - Low Damping Elastomeric Bearings and Linear Viscous Dampers
LNFS - Low Damping Elastomeric Bearings and Nonlinear Viscous Dampers
H0FS - High Damping Elastomeric Bearings (N0 Dampers)

Table 6-1: Continued

TEST	EXCITATION	PEAK TABLE MOTION			ABUTMENT						PIER				Isolation System Total Shear /Wt	DECK ACCL. (g)
		DISPL (mm)	VEL (mm/s)	ACCL. (g)	Bearing Displ. (mm)	Bearing Shear /Wt	Damper Force /Wt	Total Shear /Wt	Abut. Drift (mm)	Abut. Accl. (g)	Bearing Displ. (mm)	Pier Shear /Wt	Pier Drift (mm)	Pier Accl. (g)		
LNFS005.1	EL CENTRO S00E H+V 200%	55.9	335.	0.65	19.5	0.067	0.218	0.252	3.3	0.91	16.9	0.068	4.3	1.18	0.298	0.32
H0FS002.1	EL CENTRO S00E H+V 200%	55.4	330.	0.59	59.1	0.146	-	0.146	1.3	0.74	52.2	0.128	7.9	1.17	0.259	0.29
H0FS013.1	EL CENTRO S00E H+V 100%	28.0	171.	0.30	25.9	0.074	-	0.074	0.5	0.37	23.1	0.066	3.9	0.50	0.133	0.15
L0FS006.1	TAFT N21E 100%	16.1	78.	0.15	15.3	0.049	-	0.049	0.5	0.17	12.6	0.045	2.4	0.25	0.092	0.10
L0FS007.1	TAFT N21E 200%	32.3	158.	0.32	33.2	0.086	-	0.086	0.8	0.31	27.7	0.083	4.5	0.52	0.163	0.18
LLFS023.1	TAFT N21E 100%	16.1	77.	0.15	7.4	0.029	0.044	0.060	0.5	0.15	5.9	0.025	1.4	0.21	0.079	0.08
LLFS005.1	TAFT N21E 200%	32.4	158.	0.33	15.6	0.053	0.084	0.110	0.9	0.30	12.7	0.048	2.6	0.41	0.146	0.15
LLFS006.1	TAFT N21E 300%	48.7	237.	0.49	24.8	0.074	0.122	0.156	1.3	0.46	20.8	0.068	3.6	0.63	0.208	0.22
LLFS007.1	TAFT N21E 400%	64.9	316.	0.67	33.5	0.092	0.170	0.205	1.7	0.63	28.7	0.086	4.6	0.84	0.266	0.27
LNFS006.1	TAFT N21E 200%	28.1	130.	0.31	6.6	0.030	0.152	0.175	2.0	0.32	5.7	0.034	2.1	0.38	0.197	0.21
LNFS007.1	TAFT N21E 100%	13.8	69.	0.15	2.6	0.016	0.106	0.116	1.2	0.16	2.4	0.018	1.1	0.18	0.128	0.13
LNFS008.1	TAFT N21E 300%	42.4	198.	0.47	12.9	0.047	0.195	0.228	2.6	0.53	11.1	0.048	3.4	0.56	0.261	0.27
LNFS009.1	TAFT N21E 400%	56.4	269.	0.62	20.9	0.065	0.225	0.264	3.3	0.81	18.3	0.064	4.5	0.79	0.306	0.32
H0FS003.1	TAFT N21E 200%	27.9	129.	0.31	27.2	0.088	-	0.088	0.7	0.33	23.4	0.071	4.2	0.44	0.154	0.17
H0FS004.1	TAFT N21E 400%	56.0	254.	0.65	59.8	0.153	-	0.153	1.1	0.70	53.0	0.129	7.6	0.92	0.271	0.29
H0FS014.1	TAFT N21E 100%	13.9	66.	0.15	12.2	0.047	-	0.047	0.4	0.16	10.8	0.037	2.3	0.20	0.082	0.09
L0FS008.1	TAFT N21E H+V 200%	28.0	130.	0.31	30.2	0.080	-	0.080	1.2	0.40	25.4	0.076	4.3	0.61	0.153	0.17
LLFS008.1	TAFT N21E H+V 200% - 1	23.8	105.	0.33	8.5	0.029	0.074	0.088	0.8	0.37	7.0	0.026	2.2	0.41	0.102	0.14
LLFS008.2	TAFT N21E H+V 200% - 2	28.1	133.	0.33	15.9	0.054	0.085	0.109	1.1	0.37	13.2	0.047	3.0	0.49	0.148	0.16

Wt = Weight of the Deck = 140 kN
All Configurations are for Flexible North Pier and Stiff South Abutment
The Reported Forces at the Abutment Represent the Forces on Two Abutments
Bearing Displacements and Pier Drifts are Average Values from Two Measurements

L0FS - Low Damping Elastomeric Bearings (No Dampers)
LLFS - Low Damping Elastomeric Bearings and Linear Viscous Dampers
LNFS - Low Damping Elastomeric Bearings and Nonlinear Viscous Dampers
H0FS - High Damping Elastomeric Bearings (N0 Dampers)

Table 6-1: Continued

TEST	EXCITATION	PEAK TABLE MOTION			ABUTMENT						PIER				Isolation System Total Shear /Wt	DECK ACCL. (g)
		DISPL (mm)	VEL (mm/s)	ACCL. (g)	Bearing Displ. (mm)	Bearing Shear /Wt	Damper Force /Wt	Total Shear /Wt	Abut. Drift (mm)	Abut. Accl. (g)	Bearing Displ. (mm)	Pier Shear /Wt	Pier Drift (mm)	Pier Accl. (g)		
LLFS009.1	TAFT N21E H+V 400%	56.4	261.	0.69	36.0	0.096	0.161	0.208	3.0	0.82	30.4	0.090	6.5	1.13	0.278	0.30
LNFS010.1	TAFT N21E H+V 200%	28.1	134.	0.32	7.4	0.030	0.155	0.175	2.3	0.43	6.8	0.036	2.5	0.66	0.195	0.21
LNFS011.1	TAFT N21E H+V 400%	56.6	274.	0.66	21.5	0.067	0.221	0.248	5.4	0.97	19.0	0.073	5.7	1.16	0.288	0.36
H0FS005.1	TAFT N21E H+V 400%	56.2	263.	0.69	61.0	0.152	-	0.152	1.5	1.	54.2	0.127	8.1	1.36	0.270	0.30
H0FS015.1	TAFT N21E H+V 100%	13.9	68.	0.16	12.4	0.048	-	0.048	0.4	0.20	10.9	0.038	2.7	0.32	0.084	0.10
L0FS009.1	HACHINOHE NS 100%	31.4	134.	0.23	18.3	0.055	-	0.055	0.6	0.23	15.1	0.054	2.8	0.29	0.103	0.12
L0FS010.1	HACHINOHE NS 200%	63.1	269.	0.49	59.4	0.134	-	0.134	1.6	0.50	50.5	0.132	7.3	0.72	0.257	0.28
LLFS010.1	HACHINOHE N-S 100%	31.6	134.	0.23	13.5	0.046	0.071	0.104	0.9	0.23	11.2	0.040	2.1	0.27	0.138	0.14
LLFS011.1	HACHINOHE N-S 200%	63.2	269.	0.49	27.9	0.077	0.134	0.193	1.7	0.47	24.0	0.069	3.7	0.65	0.252	0.26
LLFS012.1	HACHINOHE N-S 300%	94.5	412.	0.78	42.9	0.105	0.205	0.291	2.8	0.74	38.1	0.095	5.5	0.94	0.378	0.38
LNFS012.1	HACHINOHE N-S 100%	31.5	144.	0.23	7.8	0.032	0.133	0.143	1.9	0.26	6.8	0.035	2.3	0.27	0.171	0.19
LNFS013.1	HACHINOHE N-S 200%	63.1	276.	0.46	21.8	0.064	0.182	0.234	3.7	0.50	19.6	0.064	4.8	0.56	0.288	0.33
LNFS014.2	HACHINOHE N-S 300%	94.4	425.	0.75	38.8	0.097	0.221	0.302	5.4	0.70	35.5	0.098	7.2	0.76	0.387	0.44
H0FS006.1	HACHINOHE NS 200%	62.8	266.	0.48	42.9	0.106	-	0.106	0.9	0.54	37.8	0.089	6.6	0.68	0.188	0.20
H0FS007.1	HACHINOHE NS 300% - 1	94.0	407.	0.75	74.8	0.170	-	0.170	1.6	0.84	66.9	0.142	8.9	1.12	0.300	0.32
H0FS007.2	HACHINOHE NS 300% - 2	94.5	412.	0.76	82.6	0.176	-	0.176	1.5	0.82	75.1	0.140	9.4	1.13	0.295	0.33
L0FS011.1	AKITA NS 100%	42.5	177.	0.24	49.6	0.115	-	0.115	1.1	0.23	42.8	0.113	6.0	0.37	0.218	0.25
LLFS013.1	AKITA N-S 100%	44.5	185.	0.25	24.3	0.070	0.101	0.142	1.3	0.24	20.6	0.062	3.5	0.28	0.192	0.21
LLFS014.1	AKITA N-S 200%	89.2	387.	0.49	51.2	0.125	0.203	0.292	2.7	0.46	44.7	0.113	6.3	0.64	0.383	0.42

Wt = Weight of the Deck = 140 kN
All Configurations are for Flexible North Pier and Stiff South Abutment
The Reported Forces at the Abutment Represent the Forces on Two Abutments
Bearing Displacements and Pier Drifts are Average Values from Two Measurements

L0FS - Low Damping Elastomeric Bearings (No Dampers)
LLFS - Low Damping Elastomeric Bearings and Linear Viscous Dampers
LNFS - Low Damping Elastomeric Bearings and Nonlinear Viscous Dampers
H0FS - High Damping Elastomeric Bearings (N0 Dampers)

Table 6-1: Continued

TEST	EXCITATION	PEAK TABLE MOTION			ABUTMENT						PIER				Isolation System Total Shear /Wt	DECK ACCL. (g)
		DISPL. (mm)	VEL (mm/s)	ACCL. (g)	Bearing Displ. (mm)	Bearing Shear /Wt	Damper Force /Wt	Total Shear /Wt	Abut. Drift (mm)	Abut. Accl. (g)	Bearing Displ. (mm)	Pier Shear /Wt	Pier Drift (mm)	Pier Accl. (g)		
LNFS015.1	AKITA N-S 100%	33.7	145.	0.18	7.4	0.031	0.123	0.137	1.5	0.22	5.7	0.030	2.1	0.22	0.161	0.17
LNFS016.1	AKITA N-S 200%	67.6	291.	0.35	23.0	0.075	0.184	0.248	3.0	0.54	19.3	0.068	4.5	0.50	0.304	0.31
H0FS008.1	AKITA NS 100%	33.7	144.	0.18	29.1	0.084	-	0.084	0.5	0.18	25.9	0.070	4.4	0.25	0.148	0.16
H0FS009.1	AKITA NS 200%	67.4	282.	0.35	71.9	0.163	-	0.163	1.2	0.36	65.3	0.132	8.5	0.59	0.279	0.32
L0FS012.1	MIYAGIKEN OKI 100%	12.0	79.	0.17	11.0	0.036	-	0.036	0.4	0.20	9.1	0.036	1.8	0.25	0.069	0.08
L0FS013.1	MIYAGIKEN OKI 200%	24.2	160.	0.36	19.1	0.056	-	0.056	0.5	0.38	16.2	0.066	3.1	0.49	0.105	0.12
L0FS014.1	MIYAGIKEN OKI 300%	36.3	236.	0.53	27.9	0.077	-	0.077	0.8	0.58	24.6	0.094	4.5	0.78	0.144	0.17
LLFS045.1	MIYAGIKEN OKI 100%	12.0	77.	0.17	4.3	0.021	0.040	0.051	0.4	0.17	3.3	0.020	1.0	0.19	0.065	0.07
LLFS046.1	MIYAGIKEN OKI 200%	24.2	157.	0.34	10.0	0.037	0.071	0.093	0.6	0.35	8.3	0.036	1.8	0.42	0.117	0.13
LLFS015.1	MIYAGIKEN OKI 300%	36.3	239.	0.51	15.0	0.046	0.104	0.127	0.9	0.53	13.2	0.043	2.4	0.66	0.153	0.17
LLFS016.1	MIYAGIKEN OKI 500%	60.6	402.	0.98	24.2	0.070	0.185	0.216	1.6	0.94	21.4	0.064	3.8	1.06	0.250	0.27
LNFS017.1	MIYAGIKEN OKI 100%	12.1	76.	0.17	2.4	0.014	0.098	0.106	1.1	0.16	2.0	0.016	1.0	0.23	0.115	0.12
LNFS018.1	MIYAGIKEN OKI 200%	24.3	148.	0.32	4.9	0.023	0.146	0.159	1.7	0.33	4.3	0.027	1.7	0.37	0.174	0.18
LNFS019.1	MIYAGIKEN OKI 300%	36.5	230.	0.49	8.7	0.034	0.180	0.197	2.3	0.46	7.7	0.041	2.1	0.54	0.220	0.23
LNFS020.1	MIYAGIKEN OKI 500%	60.9	398.	0.90	18.3	0.061	0.226	0.242	3.0	0.87	16.7	0.068	4.2	1.11	0.279	0.32
H0FS016.1	MIYAGIKEN OKI 100%	12.0	76.	0.18	7.9	0.037	-	0.037	0.3	0.21	7.2	0.029	1.7	0.22	0.064	0.08
H0FS017.1	MIYAGIKEN OKI 200%	24.3	155.	0.35	16.4	0.066	-	0.066	0.4	0.42	14.1	0.052	2.8	0.43	0.111	0.12
H0FS018.1	MIYAGIKEN OKI 300%	36.5	234.	0.54	23.4	0.079	-	0.079	0.6	0.64	21.0	0.073	4.2	0.66	0.136	0.15
H0FS019.1	MIYAGIKEN OKI 500%	60.7	394.	0.87	43.8	0.108	-	0.108	1.2	1.07	38.5	0.116	6.3	1.23	0.187	0.22

Wt = Weight of the Deck = 140 kN
All Configurations are for Flexible North Pier and Stiff South Abutment
The Reported Forces at the Abutment Represent the Forces on Two Abutments
Bearing Displacements and Pier Drifts are Average Values from Two Measurements

L0FS - Low Damping Elastomeric Bearings (No Dampers)
LLFS - Low Damping Elastomeric Bearings and Linear Viscous Dampers
LNFS - Low Damping Elastomeric Bearings and Nonlinear Viscous Dampers
H0FS - High Damping Elastomeric Bearings (N0 Dampers)

Table 6-1: Continued

TEST	EXCITATION	PEAK TABLE MOTION			ABUTMENT						PIER				Isolation System Total Shear /Wt	DECK ACCL. (g)
		DISPL (mm)	VEL (mm/s)	ACCL. (g)	Bearing Displ. (mm)	Bearing Shear /Wt	Damper Force /Wt	Total Shear /Wt	Abut. Drift (mm)	Abut. Accl. (g)	Bearing Displ. (mm)	Pier Shear /Wt	Pier Drift (mm)	Pier Accl. (g)		
L0FS015.1	PACOIMA S74W 100%	26.2	237.	0.83	50.1	0.116	-	0.116	1.3	0.91	42.8	0.119	6.2	1.22	0.221	0.26
LLFS024.1	PACOIMA S74W 50%	17.8	160.	0.55	16.7	0.053	0.093	0.113	0.8	0.51	14.0	0.046	2.7	0.70	0.155	0.16
LLFS017.1	PACOIMA S74W 100%	35.6	319.	0.97	32.4	0.087	0.177	0.208	1.7	0.95	27.7	0.080	4.8	1.41	0.276	0.29
LNFS021.1	PACOIMA S74W 100%	28.9	277.	0.79	22.1	0.069	0.211	0.236	3.2	1.05	19.9	0.087	4.8	1.11	0.274	0.31
H0FS010.1	PACOIMA S74W 100%	28.5	278.	0.86	52.0	0.110	-	0.110	0.9	1.02	47.5	0.108	5.7	1.30	0.202	0.24
L0FS016.1	PACOIMA S16E 75%	81.2	512.	0.93	97.2	0.227	-	0.227	2.8	1.11	82.6	0.226	12.0	1.64	0.433	0.48
LLFS018.1	PACOIMA S16E 75%	84.4	530.	0.92	44.6	0.110	0.263	0.284	2.3	0.96	39.0	0.105	6.5	1.06	0.340	0.35
LLFS019.1	PACOIMA S16E 100%	108.9	679.	1.16	57.7	0.138	0.356	0.351	3.5	1.15	50.8	0.128	9.1	1.66	0.431	0.43
LLFS020.1	PACOIMA S16E H+V 100%	79.0	491.	0.84	49.9	0.121	0.237	0.283	NA	0.88	46.5	0.123	NA	1.27	0.387	0.41
LNFS022.1	PACOIMA S16E 100%	79.7	492.	0.88	56.6	0.139	0.245	0.346	5.7	1.06	49.0	0.140	8.3	1.53	0.458	0.51
LNFS023.1	PACOIMA S16E H+V 100%	79.4	507.	0.91	50.8	0.122	0.256	0.339	NA	1.19	48.4	0.193	NA	1.80	0.455	0.50
H0FS011.1	PACOIMA S16E 100%	78.9	493.	0.94	106.0	0.234	-	0.234	2.2	1.23	95.5	0.204	11.8	1.40	0.414	0.46
L0FS017.1	JP LEVEL 2 GC 1 75%	80.2	344.	0.29	86.0	0.204	-	0.204	1.8	0.30	74.6	0.188	9.9	0.35	0.379	0.42
LLFS021.1	JP LEVEL 2 G.C. 1 75%	80.9	350.	0.29	32.4	0.087	0.130	0.176	1.3	0.36	27.8	0.081	4.6	0.35	0.234	0.25
LLFS022.1	JP LEVEL 2 G.C. 1 100%	107.5	469.	0.39	45.3	0.112	0.181	0.237	1.9	0.43	38.9	0.104	6.1	0.45	0.304	0.33
LNFS024.1	JP LEVEL 2 G.C. 1 75%	81.1	358.	0.32	17.8	0.059	0.165	0.181	2.5	0.43	15.3	0.063	4.0	0.42	0.224	0.26
LNFS025.1	JP LEVEL 2 G.C. 1 100%	108.2	478.	0.41	29.5	0.085	0.200	0.253	3.3	0.66	25.2	0.090	5.9	0.56	0.307	0.34
H0FS023.1	JP LEVEL 2 GC 1 100%	107.9	469.	0.41	84.8	0.216	-	0.216	1.4	0.44	78.6	0.160	10.0	0.54	0.353	0.39
LNFS026.1	JP LEVEL 2 G.C. 2 50%	50.4	224.	0.19	11.1	0.041	0.144	0.171	1.9	0.28	9.0	0.042	3.1	0.27	0.200	0.21

Wt = Weight of the Deck = 140 kN
All Configurations are for Flexible North Pier and Stiff South Abutment
The Reported Forces at the Abutment Represent the Forces on Two Abutments
Bearing Displacements and Pier Drifts are Average Values from Two Measurements

L0FS - Low Damping Elastomeric Bearings (No Dampers)
LLFS - Low Damping Elastomeric Bearings and Linear Viscous Dampers
LNFS - Low Damping Elastomeric Bearings and Nonlinear Viscous Dampers
H0FS - High Damping Elastomeric Bearings (N0 Dampers)

Table 6-1: Continued

TEST	EXCITATION	PEAK TABLE MOTION			ABUTMENT						PIER				Isolation System Total Shear /Wt	DECK ACCL. (g)	
		DISPL (mm)	VEL (mm/s)	ACCL. (g)	Bearing Displ. (mm)	Bearing Shear /Wt	Damper Force /Wt	Total Shear /Wt	Abut. Drift (mm)	Abut. Accl. (g)	Bearing Displ. (mm)	Pier Shear /Wt	Pier Drift (mm)	Pier Accl. (g)			
LNFS027.1	JP LEVEL 2 G.C. 2 100%	100.9	457.	0.40	37.5	0.109	0.226	0.312	3.9	0.53	32.7	0.106	7.4	0.47	0.395	0.41	
H0FS024.1	JP LEVEL 2 GC 2 100%	100.9	455.	0.42	82.5	0.148	-	0.148	1.4	0.46	75.5	0.123	8.2	0.62	0.253	0.29	
LNFS028.1	JP LEVEL 2 G.C. 3 75%	82.7	372.	0.32	19.4	0.061	0.194	0.212	3.4	0.48	16.7	0.065	4.6	0.46	0.261	0.27	
LNFS029.1	JP LEVEL 2 G.C. 3 100%	109.9	507.	0.52	32.9	0.090	0.225	0.280	11.5	0.65	28.5	0.092	6.5	0.60	0.353	0.37	
H0FS025.1	JP LEVEL 2 GC 3 100%	109.6	509.	0.55	131.7	0.301	-	0.301	2.3	0.57	123.4	0.211	12.4	0.75	0.484	0.54	*
L0FS018.1	JP LEVEL 1 GC 1 100%	16.1	95.	0.11	22.7	0.063	-	0.063	0.6	0.11	19.0	0.058	3.0	0.14	0.120	0.13	
LLFS025.1	JP LEVEL 1 G.C. 1 100%	16.3	97.	0.11	9.0	0.036	0.042	0.068	0.5	0.13	7.3	0.031	1.8	0.13	0.095	0.10	
LNFS030.1	JP LEVEL 1 G.C. 1 100%	16.4	109.	0.11	3.4	0.019	0.100	0.108	1.1	0.16	2.8	0.020	1.1	0.13	0.118	0.12	
H0FS020.1	JP LEVEL 1 GC 1 100%	16.2	100.	0.11	17.5	0.064	-	0.064	0.5	0.11	15.1	0.051	3.0	0.16	0.109	0.12	
L0FS021.1	JP LEVEL 1 GC 2 100%	17.1	114.	0.12	30.4	0.079	-	0.079	0.7	0.13	25.8	0.077	4.0	0.17	0.150	0.17	
LLFS026.1	JP LEVEL 1 G.C. 2 100%	17.3	114.	0.12	11.6	0.039	0.054	0.079	0.6	0.13	9.4	0.034	1.9	0.15	0.108	0.12	
LNFS031.1	JP LEVEL 1 G.C. 2 100%	17.6	117.	0.12	4.2	0.019	0.099	0.109	1.2	0.15	3.1	0.022	1.4	0.16	0.118	0.13	
H0FS021.1	JP LEVEL 1 GC 2 100%	17.5	119.	0.12	24.4	0.077	-	0.077	0.5	0.13	21.3	0.065	3.9	0.15	0.134	0.15	
L0FS019.1	JP LEVEL 1 GC 3 100%	33.4	156.	0.13	40.5	0.097	-	0.097	0.9	0.13	34.2	0.096	5.2	0.16	0.186	0.20	
LLFS027.1	JP LEVEL 1 G.C. 3 100%	33.5	158.	0.13	11.8	0.039	0.055	0.077	0.6	0.13	9.7	0.035	1.9	0.16	0.108	0.12	
LNFS032.1	JP LEVEL 1 G.C. 3 100%	33.3	294.	0.14	4.5	0.022	0.111	0.111	NA	0.17	3.8	0.023	NA	0.24	0.119	0.13	
H0FS022.1	JP LEVEL 1 GC 3 100%	33.4	159.	0.13	23.7	0.074	-	0.074	0.5	0.13	20.6	0.062	3.7	0.15	0.130	0.14	
L0FS020.1	NORTHRIDGE SYL. 90° 100%	49.8	339.	0.58	83.6	0.179	-	0.179	2.1	0.57	71.7	0.179	9.9	0.57	0.348	0.38	
LLFS028.1	NORTHRIDGE SYLMAR 90° 50%	24.9	167.	0.30	18.4	0.059	0.081	0.120	1.0	0.34	15.4	0.052	2.9	0.25	0.168	0.17	

Wt = Weight of the Deck = 140 kN
All Configurations are for Flexible North Pier and Stiff South Abutment
The Reported Forces at the Abutment Represent the Forces on Two Abutments
Bearing Displacements and Pier Drifts are Average Values from Two Measurements

* Failure of SW Elastomeric Bearing

L0FS - Low Damping Elastomeric Bearings (No Dampers)
LLFS - Low Damping Elastomeric Bearings and Linear Viscous Dampers
LNFS - Low Damping Elastomeric Bearings and Nonlinear Viscous Dampers
H0FS - High Damping Elastomeric Bearings (N0 Dampers)

Table 6-1: Continued

TEST	EXCITATION	PEAK TABLE MOTION			ABUTMENT						PIER				Isolation System Total Shear /Wt	DECK ACCL. (g)
		DISPL (mm)	VEL (mm/s)	ACCL. (g)	Bearing Displ. (mm)	Bearing Shear /Wt	Damper Force /Wt	Total Shear /Wt	Abut. Drift (mm)	Abut. Accl. (g)	Bearing Displ. (mm)	Pier Shear /Wt	Pier Drift (mm)	Pier Accl. (g)		
LLFS029.1	NORTHRIDGE SYLMAR 90° 75%	37.4	251.	0.44	29.1	0.081	0.117	0.170	1.5	0.47	24.6	0.073	4.1	0.37	0.237	0.24
LLFS030.1	NORTHRIDGE SYL. 90° 100%	49.8	340.	0.60	39.4	0.101	0.158	0.222	2.1	0.62	33.7	0.093	5.2	0.51	0.301	0.31
LNFS033.1	NORTHRIDGE SYL. 90° 100%	50.4	344.	0.63	34.7	0.093	0.202	0.265	NA	0.84	30.5	0.098	6.5	0.58	0.348	0.38
LNFS034.1	NORTHRIDGE SYL. 90° 150%	75.5	517.	0.99	62.7	0.150	0.236	0.361	5.9	1.28	54.8	0.143	9.8	0.87	0.490	0.54
L0FS022.1	NORTHRIDGE Syl. 90° H+V 100%	49.8	341.	0.59	86.6	0.187	-	0.187	2.6	0.68	74.2	0.187	11.0	0.86	0.362	0.40
LLFS031.1	NORTHRIDGE Syl. 90° H+V 100%	49.7	344.	0.62	40.1	0.104	0.155	0.216	1.9	0.66	33.9	0.097	6.4	0.83	0.300	0.31
LNFS035.1	NORTHRIDGE Syl. 90° H+V 100%	50.5	356.	0.64	34.9	0.091	0.203	0.264	4.3	0.78	31.5	0.110	7.4	1.11	0.350	0.38
LNFS036.1	NORTHRIDGE Syl. 90° H+V 150%	75.4	534.	1.	62.8	0.149	0.236	0.360	6.7	1.48	55.6	0.172	12.2	1.43	0.491	0.53
LLFS032.1	NORTHRIDGE Newhall 90° 100%	43.6	311.	0.99	24.6	0.067	0.145	0.183	1.6	0.94	21.4	0.060	3.7	1.22	0.232	0.24
L0FS023.1	NORTHRIDGE NH 90° H+V 100%	43.2	329.	0.90	57.8	0.133	-	0.133	1.9	1.01	50.8	0.157	8.4	1.63	0.262	0.30
LLFS033.1	NORTHRIDGE NH 90° H+V 100%	43.5	323.	0.96	24.3	0.066	0.168	0.189	2.6	1.02	21.4	0.059	5.1	1.34	0.219	0.29
L0FS025.1	NORTHRIDGE Newhall 360° 75%	43.5	322.	0.61	68.6	0.147	-	0.147	1.6	0.65	58.7	0.153	8.1	0.79	0.285	0.31
LLFS034.1	NORTHRIDGE Newhall360° 50%	29.4	208.	0.37	20.3	0.056	0.127	0.161	1.3	0.36	18.0	0.051	2.8	0.43	0.205	0.22
LLFS035.1	NORTHRIDGE Newhall 360° 75%	44.1	322.	0.60	28.9	0.076	0.200	0.246	2.1	0.58	26.2	0.068	4.1	0.72	0.300	0.32
LLFS036.1	NORTHRIDGE Newhall 360° 100%	58.9	438.	0.85	38.2	0.098	0.279	0.332	2.8	0.81	32.8	0.090	5.5	1.06	0.393	0.42
LNFS037.1	NORTHRIDGE Newhall 360° 100%	59.4	451.	0.81	38.3	0.094	0.241	0.324	4.0	0.94	35.7	0.111	5.8	1.20	0.409	0.43
LLFS037.1	NORTHRIDGE NH 360°H+V100%	58.8	454.	0.86	40.8	0.108	0.284	0.334	3.5	1.	37.2	0.107	8.7	1.50	0.384	0.39

Wt = Weight of the Deck = 140 kN
All Configurations are for Flexible North Pier and Stiff South Abutment
The Reported Forces at the Abutment Represent the Forces on Two Abutments
Bearing Displacements and Pier Drifts are Average Values from Two Measurements

L0FS - Low Damping Elastomeric Bearings (No Dampers)
LLFS - Low Damping Elastomeric Bearings and Linear Viscous Dampers
LNFS - Low Damping Elastomeric Bearings and Nonlinear Viscous Dampers
H0FS - High Damping Elastomeric Bearings (N0 Dampers)

Table 6-1: Continued

TEST	EXCITATION	PEAK TABLE MOTION			ABUTMENT						PIER				Isolation System Total Shear /Wt	DECK ACCL. (g)
		DISPL (mm)	VEL (mm/s)	ACCL. (g)	Bearing Displ. (mm)	Bearing Shear /Wt	Damper Force /Wt	Total Shear /Wt	Abut. Drift (mm)	Abut. Accl. (g)	Bearing Displ. (mm)	Pier Shear /Wt	Pier Drift (mm)	Pier Accl. (g)		
LNFS038.1	NORTHRIDGE NH 360°H+V100%	59.6	426.	0.78	38.9	0.096	0.248	0.318	5.3	1.11	34.4	0.120	8.0	1.64	0.396	0.44
L0FS024.1	KOBE - KOBE STATION NS 100%	41.7	445.	0.81	93.5	0.224	-	0.224	2.8	0.80	80.8	0.238	11.6	1.28	0.411	0.47
LLFS038.1	KOBE - KOBE STATION N-S 50%	21.1	210.	0.38	18.1	0.054	0.148	0.162	1.3	0.36	15.7	0.048	2.5	0.40	0.181	0.20
LLFS039.1	KOBE - KOBE STATION NS 100%	42.4	450.	0.86	35.7	0.085	0.311	0.344	2.8	0.80	33.3	0.081	5.9	1.21	0.377	0.41
LNFS039.1	KOBE - KOBE STATION NS 100%	42.4	448.	0.77	37.6	0.094	0.256	0.322	4.1	1.14	34.4	0.094	5.8	0.97	0.394	0.44
LLFS040.1	KOBE - KOBE ST. N-S H+V 100%	43.1	443.	0.93	37.3	0.095	0.310	0.342	4.1	0.91	33.7	0.089	8.1	1.45	0.391	0.38
LNFS040.1	KOBE - KOBE ST. N-S H+V 100%	42.3	455.	0.83	36.2	0.082	0.258	0.324	5.0	1.18	33.9	0.102	6.0	1.58	0.392	0.41
LLFS041.1	MEXICO CITY N90W 50%	25.0	145.	0.09	15.7	0.050	0.051	0.081	0.7	0.10	12.8	0.044	2.6	0.11	0.120	0.13
LLFS042.1	MEXICO CITY N90W 60%	30.0	175.	0.12	20.2	0.061	0.063	0.099	0.9	0.12	16.6	0.054	3.1	0.15	0.145	0.15
LLFS043.1	MEXICO CITY N90W 80%	40.0	234.	0.15	30.0	0.082	0.086	0.134	1.3	0.15	25.1	0.074	4.4	0.16	0.195	0.21
LLFS044.1	MEXICO CITY N90W 100%	52.2	305.	0.18	42.3	0.106	0.121	0.175	1.8	0.18	35.7	0.097	5.8	0.25	0.254	0.27
LNFS041.1	MEXICO CITY N90W 100%	52.1	309.	0.19	14.2	0.050	0.131	0.159	2.7	0.20	11.9	0.049	3.9	0.22	0.193	0.21

Wt = Weight of the Deck = 140 kN
All Configurations are for Flexible North Pier and Stiff South Abutment
The Reported Forces at the Abutment Represent the Forces on Two Abutments
Bearing Displacements and Pier Drifts are Average Values from Two Measurements

L0FS - Low Damping Elastomeric Bearings (No Dampers)
LLFS - Low Damping Elastomeric Bearings and Linear Viscous Dampers
LNFS - Low Damping Elastomeric Bearings and Nonlinear Viscous Dampers
H0FS - High Damping Elastomeric Bearings (N0 Dampers)

Testing of the isolated bridge was conducted with a number of records from the 1994 Northridge and 1995 Japanese Kobe earthquakes. These records together with some from the 1971 San Fernando earthquake were characterized by near-fault conditions with high ground velocity. Unfortunately, testing of the high damping elastomeric isolation system was not conducted with the Northridge and Kobe motions due to failure of the bearings.

It is important to note in Table 6-1 that the peak table motion is not the same for motions that were specified to be identical. The reasons for this phenomenon were the table-structure interaction and the occasionally insufficient hydraulic power in the stronger inputs (which was affected by the demand for power from the other experiments conducted in the laboratory at the same time). Due to the long-period characteristics of the tested isolated bridge, the relevant parameter for assessing the intensity of the seismic input is the peak table velocity.

6.3 Interpretation of Results

6.3.1 Behavior of High Damping Elastomeric System under Unscragged and Scragged Conditions

The high damping elastomeric bearings were installed in the bridge model without prior testing. Accordingly, they exhibited unscragged properties. As evaluated in Section 4 from the testing of another bearing, the unscragged conditions were characterized by a stiffness approximately 50-percent higher than the scragged one. It has been assumed that the scragged properties are not stable and that recovery to the unscragged properties occurs after some time. Accordingly, repetitive testing with the same strong excitation was conducted. The interest was to observe the bearing displacement response and the force transferred to the substructure under scragged conditions and under conditions following recovery (presumed to be the same as the unscragged conditions).

Testing with the El Centro S00E (horizontal component only) motion scaled up by factor 2.0 (denoted in Table 6-1 as El Centro S00E 200%) was conducted first. The same test was repeated two more times, it was followed by four other tests, and then again repeated twice. Figure 6-1 presents the force-displacement loops of the southwest abutment and the northwest flexible pier bearings recorded in the first (unscragged), third and fifth tests in this sequence. These graphs, together with the results in Table 6-1, demonstrate that during the scragging process there is a substantial drop in the effective stiffness of the isolation system from about 0.83 kN/mm in the first test to about 0.54 kN/mm in the fifth test (indeed as determined in the testing of the first bearing, the unscragged stiffness is about 50-percent larger than the scragged stiffness). Moreover, there is a reduction in the characteristic strength of the system, from about 10.5 kN in the first test to about 8.9 kN in the fifth test.

In terms of the displacement response, we observe a minor difference between the unscragged and scragged conditions. As seen in Table 6-1, under unscragged bearing conditions (test H0FS001.1) the bearing displacements are about 15-percent less than the displacements under scragged bearing conditions. However, there is a marked difference in the force transmitted to the

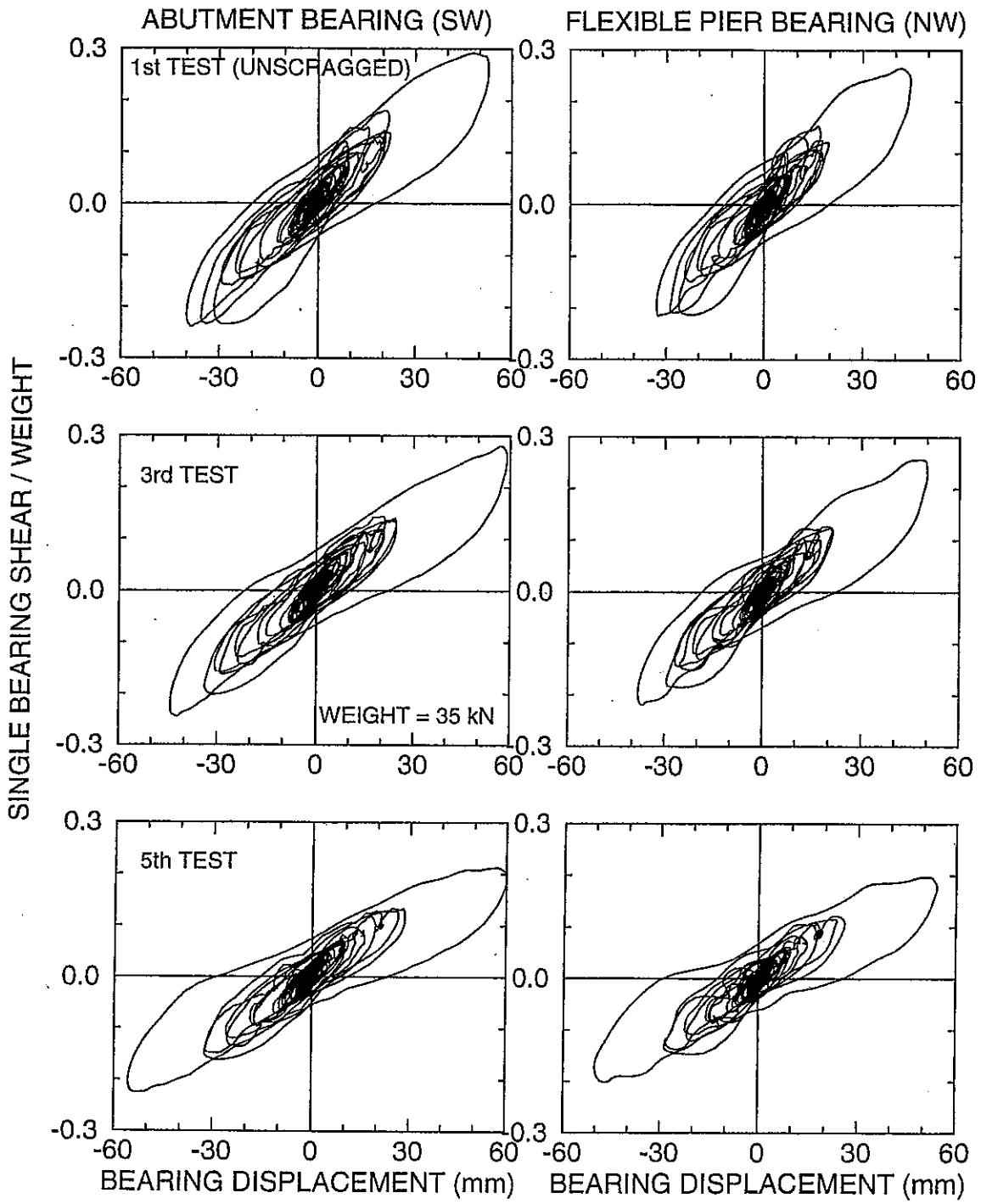

Figure 6-1: Comparison of Force-Displacement Loops of High Damping Elastomeric Bearings in Repetitive Testing with El Centro S00E 200% Input

substructure. As seen in Table 6-1, the peak total shear force in the isolation system changes from 0.284 to 0.212 times the deck weight. That is, the force transmitted to the substructure under unscragged conditions is about 30-percent higher than the force transmitted under scragged conditions.

Of interest is to note that the observed differences are entirely predictable on the basis of the simple equations in the 1997 AASHTO (American Association of State Highway and Transportation Officials, 1997). Specifically, the isolation system displacement, d, and the isolation system force, F are related to the effective period, T_{eff}, and damping coefficient, B (which is related to the effective damping) by:

$$d \sim \frac{T_{eff}}{B} \tag{6-1}$$

$$F \sim \frac{1}{BT_{eff}} \tag{6-2}$$

where the symbol ~ denotes proportionality. For the tested system the following parameters were determined from the experimental data. For unscragged conditions (first test): $T_{eff} = 0.83$ *sec*, $\beta = 0.16$, $B = 1.38$. For scragged conditions (fifth test): $T_{eff} = 1.02$ *sec*, $\beta = 0.18$, $B = 1.44$.

Assigning subscripts s for the scragged conditions and u for the unscragged conditions, we have on the basis of (6-1) and (6-2):

$$\frac{d_s - d_u}{d_s} = 1 - \frac{T_{effu} \cdot B_s}{T_{effs} \cdot B_u} \tag{6-3}$$

$$\frac{F_u - F_s}{F_s} = \frac{B_s \cdot T_{effs}}{B_u \cdot T_{effu}} - 1 \tag{6-4}$$

For the tested system, (6-3) gives 0.15 and (6-4) gives 0.28, that is, in good agreement with the experiments.

We conclude that analysis of isolated structures on the basis of the scragged properties of high damping bearings may underestimate the isolation system forces by a significant amount when comparing to the conditions of the bearings after some time in service (herein we presume that the bearings recover their unscragged properties).

6.3.2 Comparison of Behavior of Non-isolated and Isolated Bridge Configurations without Dampers

Figure 6-2 presents a comparison of key response quantities of the non-isolated and the isolated bridge configurations without dampers. These response quantities are presented as functions of the peak table velocity, which is an appropriate measure of intensity of the seismic input for the

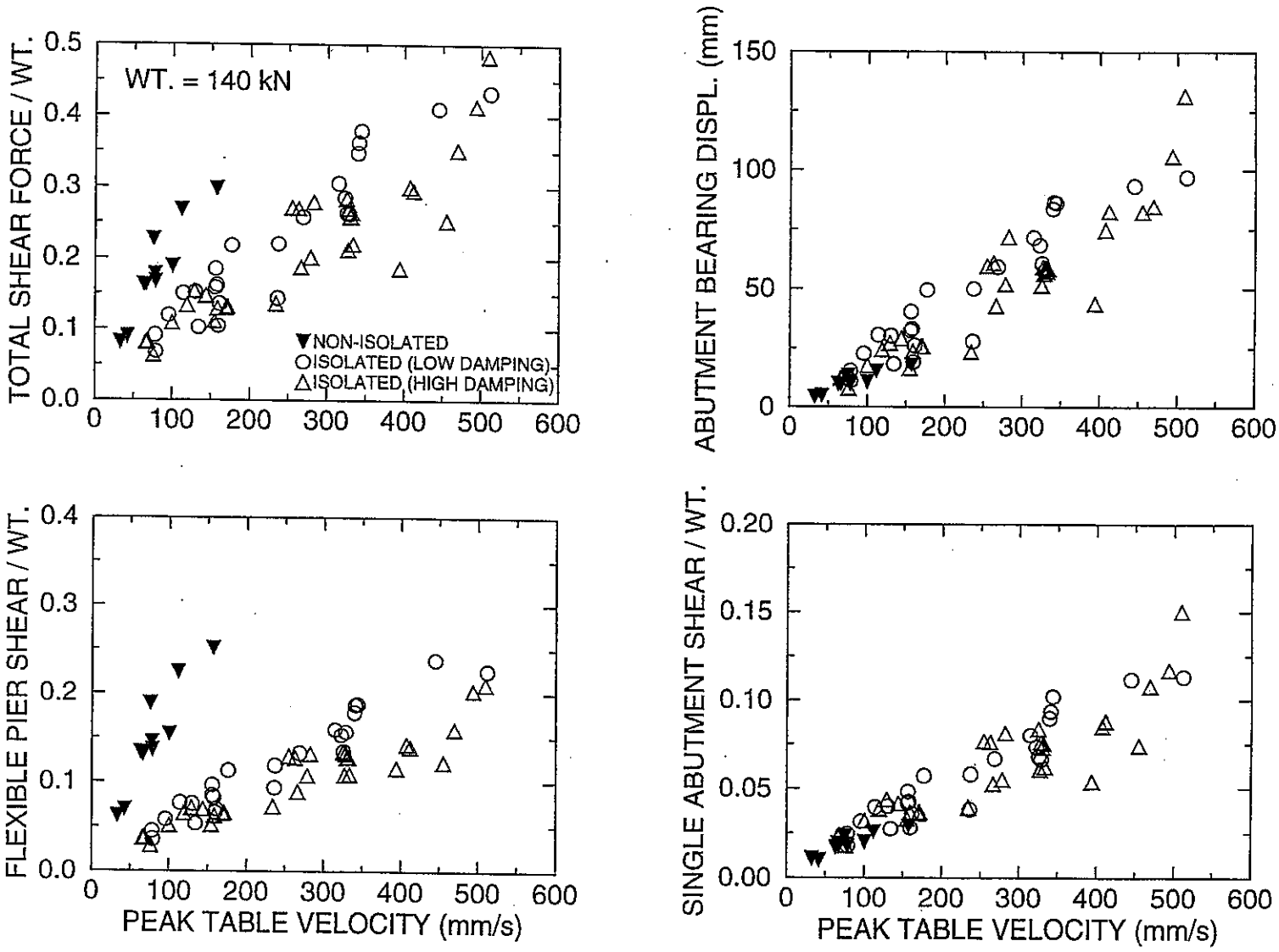

Figure 6-2: Comparison of Peak Response of Non-isolated and Isolated Bridge Configurations without Dampers

tested flexible systems. This figure clearly demonstrates the effects of isolation: reduction of the shear force transmitted to the vulnerable pier at the expense of larger bearing displacements and accordingly larger force transmitted to the abutments.

However, the interesting result in this figure is that the response of the isolated bridge with low damping elastomeric bearings is, in many tests, not very different from the response of the high damping elastomeric system. One would expect an overall superior performance from the high damping elastomeric system given that the two systems had essentially the same effective period but substantially different effective damping (less than 0.09 in the low damping system versus about 0.15 to 0.20 for the high damping system).

Accordingly, we proceed with a direct comparison of response of the low and high damping elastomeric systems under the same seismic excitation. Figures 6-3 to 6-6 present comparisons of time histories of the abutment bearing displacements, isolation system shear force versus bearing displacement loops and the flexible pier shear force versus pier drift loops in the tests with the Hachinohe NS 200%, El Centro S00E 200%, Japanese Level 1 and Ground Condition 3 (soft soil) 100%, and Pacoima Dam S74W 100% horizontal seismic input.

Starting with Figure 6-3 we observe the benefits offered by the high damping elastomeric system. There is a reduction in bearing displacement which is consistent with equation (6-1). That is, when considering an effective damping of about 7 to 8-percent for the low damping system (so that $B \approx 1.10$) and effective damping of about 15 to 20-percent for the high damping system (so that $B \approx 1.45$), we expect a ratio of peak displacement in the two systems of about $1.10/1.45 \approx 0.75$ provided that the effective period is the same.

In the case of the El Centro input (Figure 6-4) there is very little difference in the displacement response of the two systems due to the larger effective period of the high damping elastomeric system. However, the benefit of reduction of the force transmitted to the substructure is evident.

The great benefit of increased damping is seen in the case of the Japanese Level 1, ground condition 3 input (Figure 6-5). Due to the existence of strong, long period components in this input the two systems are essentially driven to resonance. Accordingly, the high damping system shows a clearly superior performance which can not be predicted on the basis of equation (6-1). For such a case, the ratio of peak displacements may be approximately calculated by

$$\frac{d_h}{d_l} \approx \frac{\beta_l}{\beta_h} \tag{6-5}$$

where the subscripts h and l denote high damping and low damping systems, respectively, and β is the effective damping. Equation (6-5) is based on the known displacement magnification relation at resonance of harmonically excited systems (Chopra, 1995). Approximately for the two systems in Figure 6-5, $\beta_l = 0.08$ and $\beta_h = 0.15$. Accordingly, (6-5) results in $d_h/d_l \approx 0.53$, which is consistent with the experimental results.

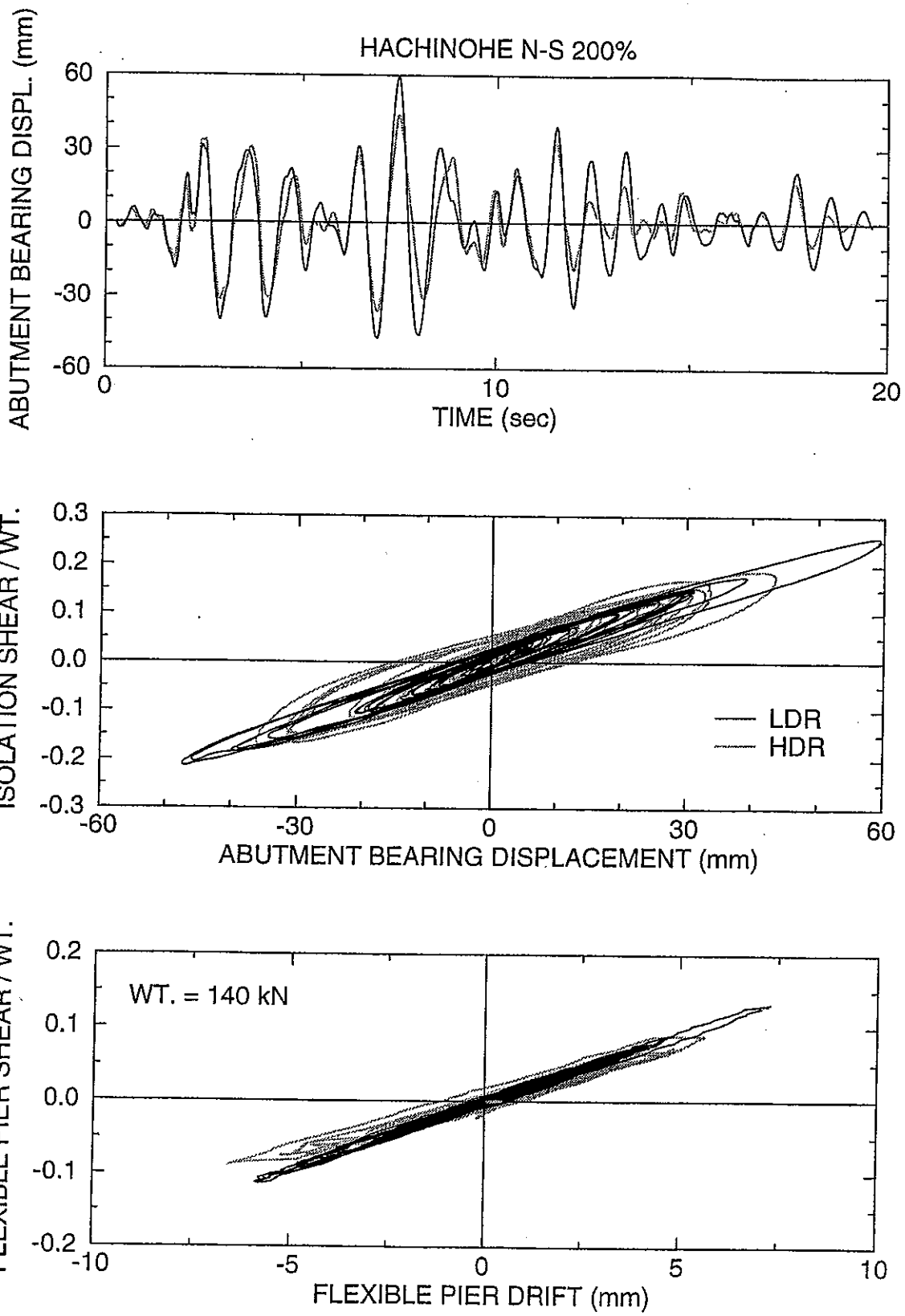

Figure 6-3: Comparison of Response of Isolated Bridge with Elastomeric Systems for Hachinohe N-S 200% Input

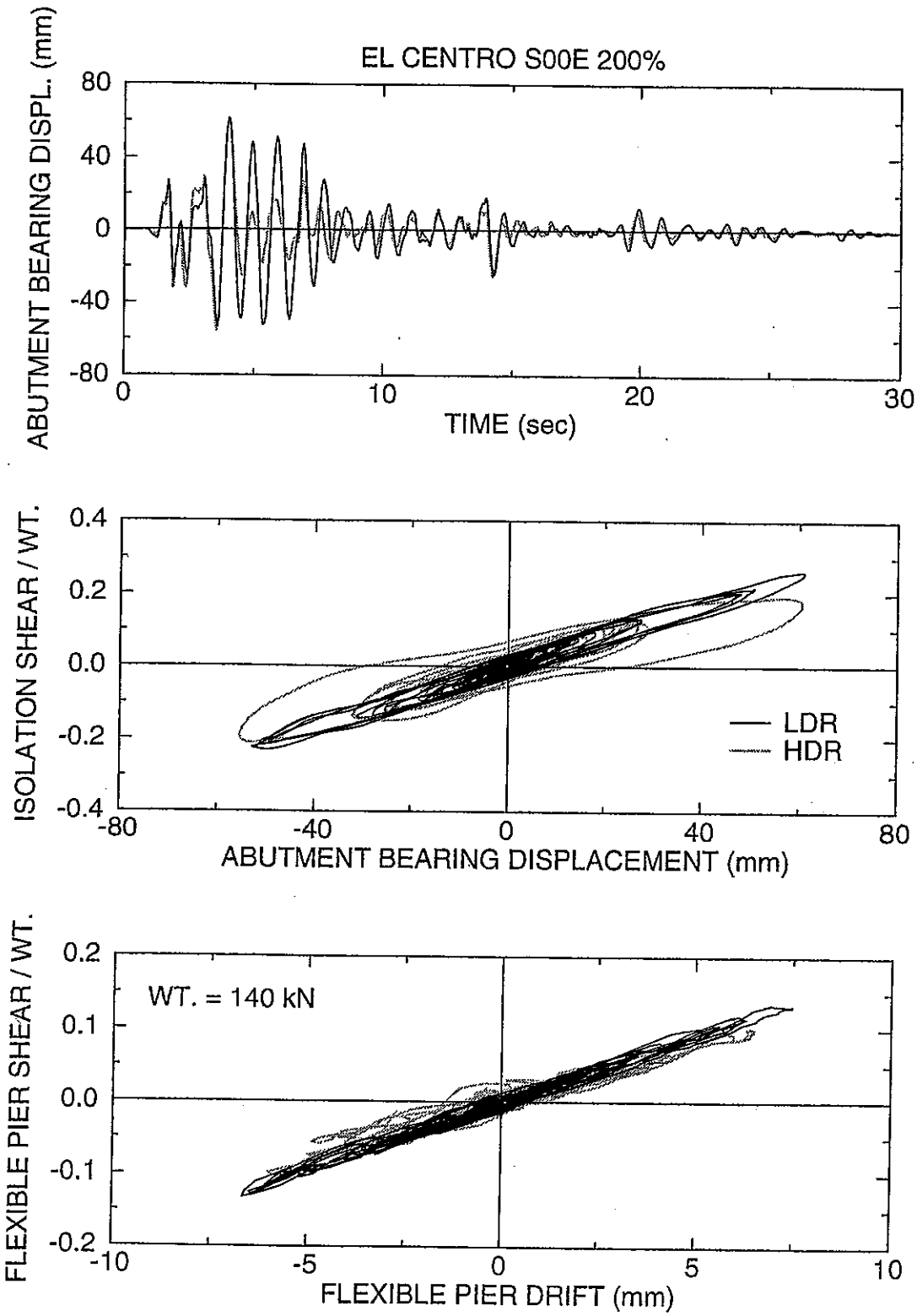

Figure 6-4: Comparison of Response of Isolated Bridge with Elastomeric Systems for El Centro S00E 200% Input

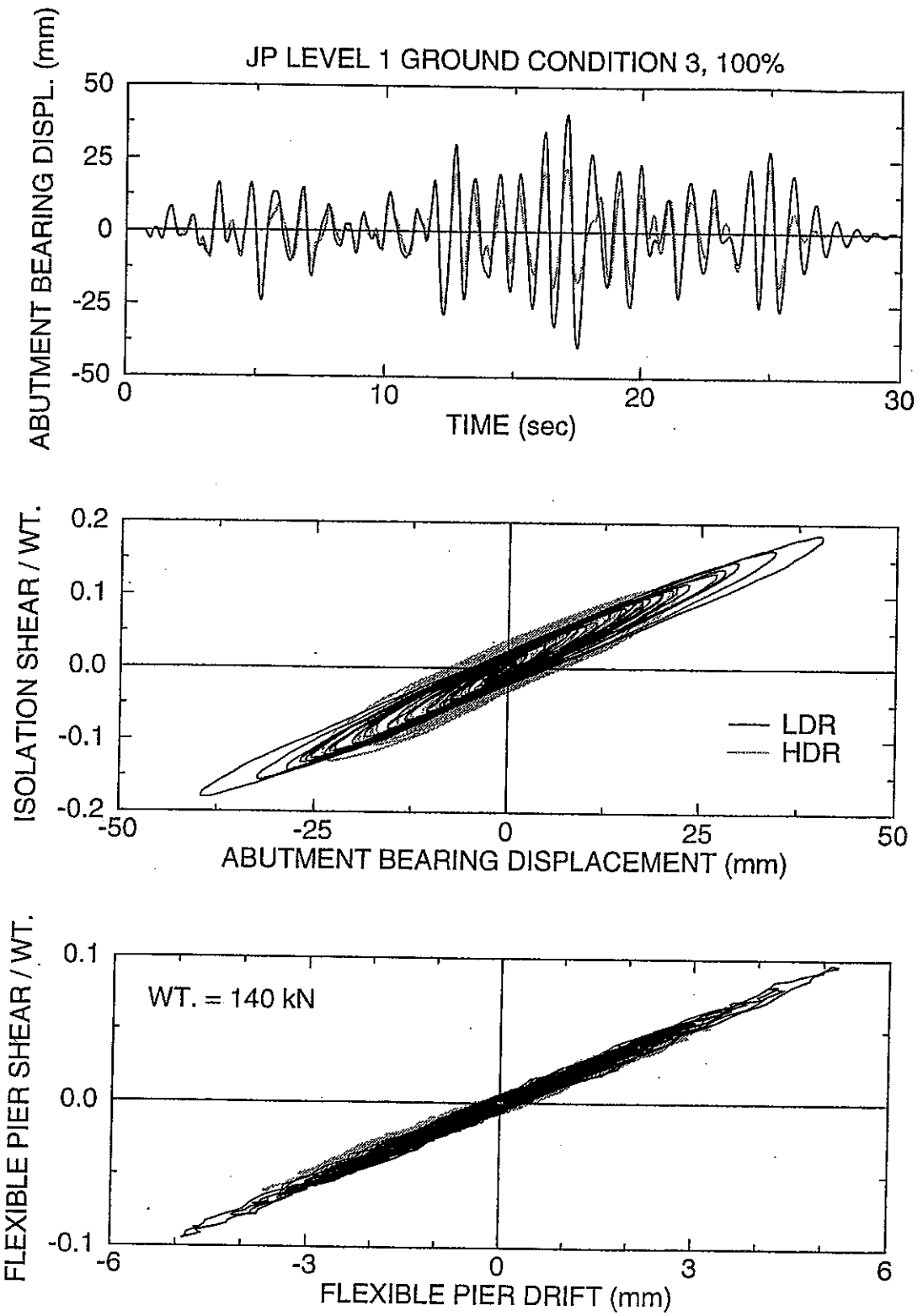

Figure 6-5: Comparison of Response of Isolated Bridge with Elastomeric Systems for Japanese Level 1, Ground Condition 3, 100% Input

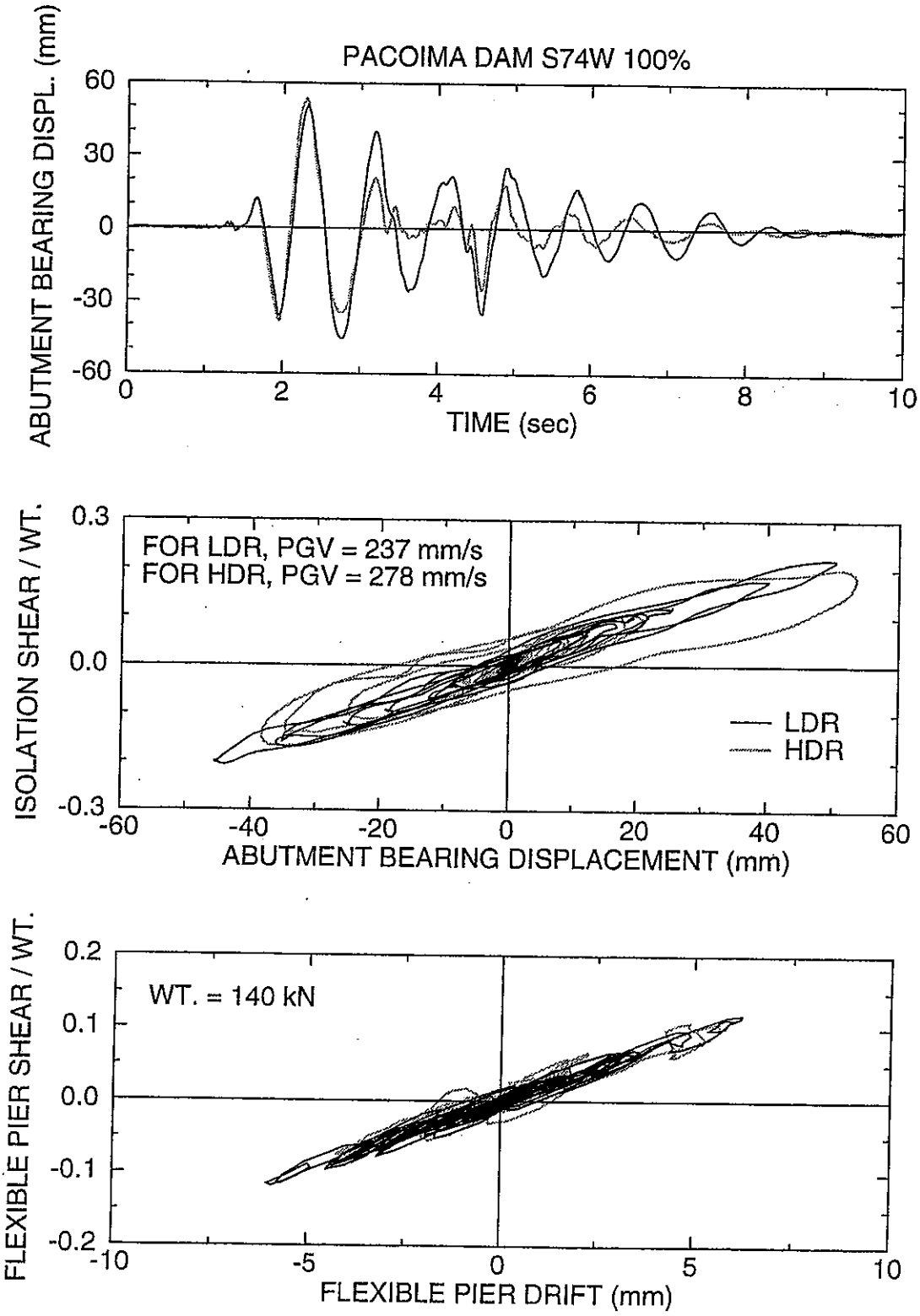

Figure 6-6: Comparison of Response of Isolated Bridge with Elastomeric Systems for Pacoima Dam S74W 100% Input

Finally, we discuss the case of the Pacoima Dam S74W input (Figure 6-6). To start, we note that the inputs in the two tests differed in terms of the peak table velocity (278 mm/s in the high damping system and 237 mm/s in the low damping system). If we approximately adjust the displacement of the low damping system to correspond to the input of 278 mm/s peak table velocity, we obtain an abutment bearing displacement of nearly 59 mm versus the 52 mm measured displacement of the high damping system. There is, therefore, some benefit offered by the high damping system in reducing the displacements. However, the benefit is not as large as in other types of input. We recognize the near-fault characteristics of this input (however, not as prevalent as in other inputs), which will be further discussed later in this report.

Unfortunately, testing of the high damping elastomeric system was not conducted with other motions having prevalent near-fault characteristics due to failure of one of high damping elastomeric bearings. However, we could obtain a very good set of results when we tested the two systems with the Pacoima Dam record, component S16E. This motion contained a clear high velocity shock. The two systems were tested for different specified intensities of this input (see Table 6-1) but for some unknown reason the motion of the table was nearly identical. Figure 6-7 presents a comparison of the recorded response in the two tests (tests L0FS016.1 and H0FS011.1). The inputs are nearly the same with the low damping system excited by slightly higher peak velocity. It may be observed that the two systems experienced nearly the same peak bearing displacements and peak force in the isolation system. The higher damping did not have any effect during the cycle of movement caused by the input velocity shock. However, it had a substantial effect during the subsequent cycles (which were essentially cycles of free vibration response).

Concluding, we note that the high damping elastomeric bearings were effective in the reduction of displacement and accordingly force in the structure in motions lacking high velocity shocks which are characteristics of near-fault motions. This issue will be further discussed when the results of testing of the system with added viscous dampers are presented.

6.3.3 Failure of Elastomeric Bearings

During the testing of the high damping elastomeric system with the Japanese level 2 and ground condition 3 (soft soil) input (test No. H0FS025.1), the southwest abutment bearing failed. Figure 6-8 presents plots of the force displacement loops of the four bearings during this test.

The displacements of the bearings reached rubber shear strains of about 175-percent for which the bearings were theoretically unstable. However, the bearings appeared stable and exhibited some stiffening at large strains (beyond approximately 120-percent) which was characteristic of the utilized rubber compound. The bearing at the southwest side on top of the abutment failed in a combined de-bonding of rubber from the top end plate and fracture of rubber in the top layer. It was bearing No. 3 from batch No. 1 which was likely improperly cured and exhibited significant creep. The fact that the failure initiated as de-bonding of the rubber from the steel plate further reinforces the notion of improper curing.

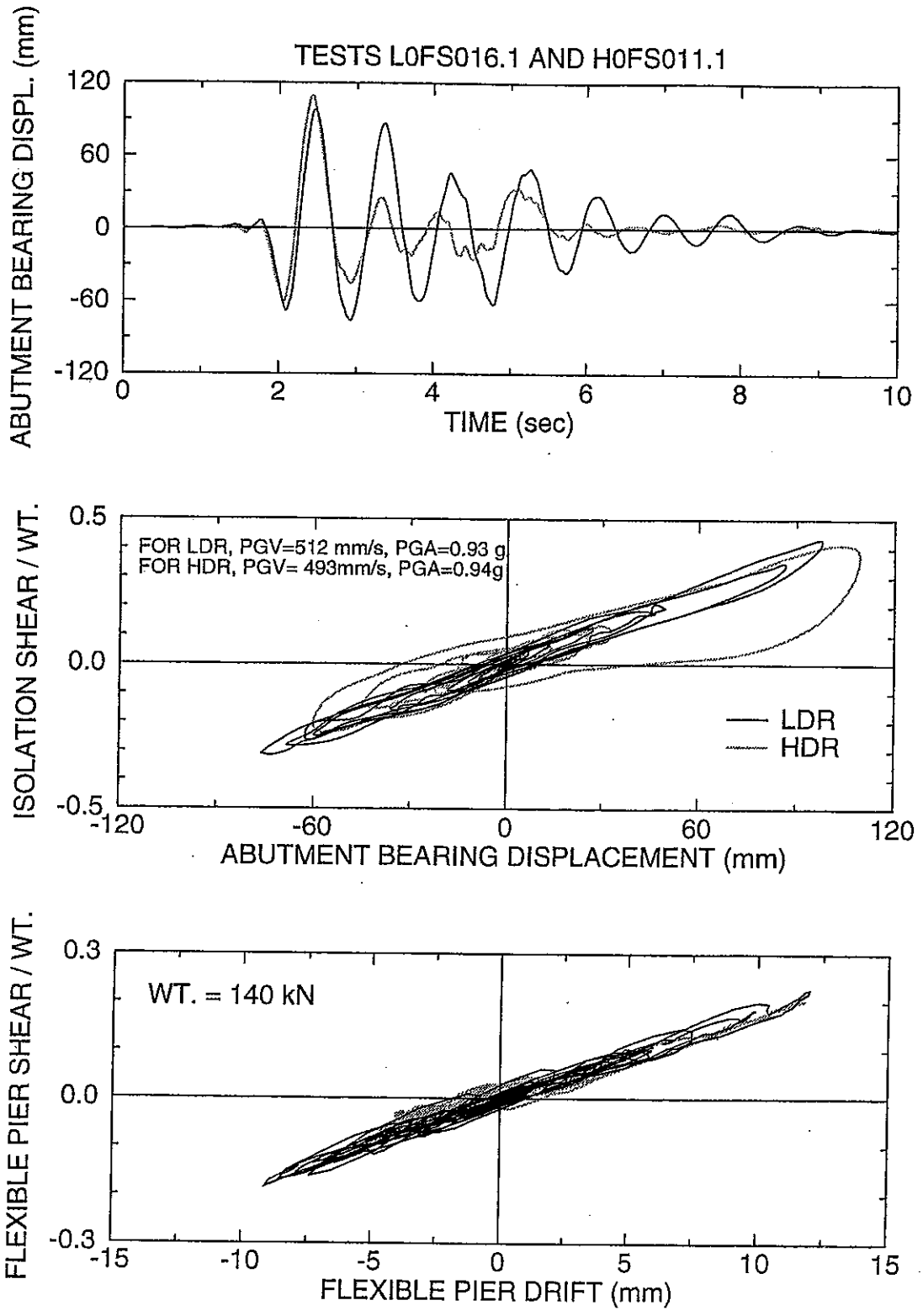

Figure 6-7: Comparison of Response of Isolated Bridge with Elastomeric Systems for Pacoima Dam S16E Input

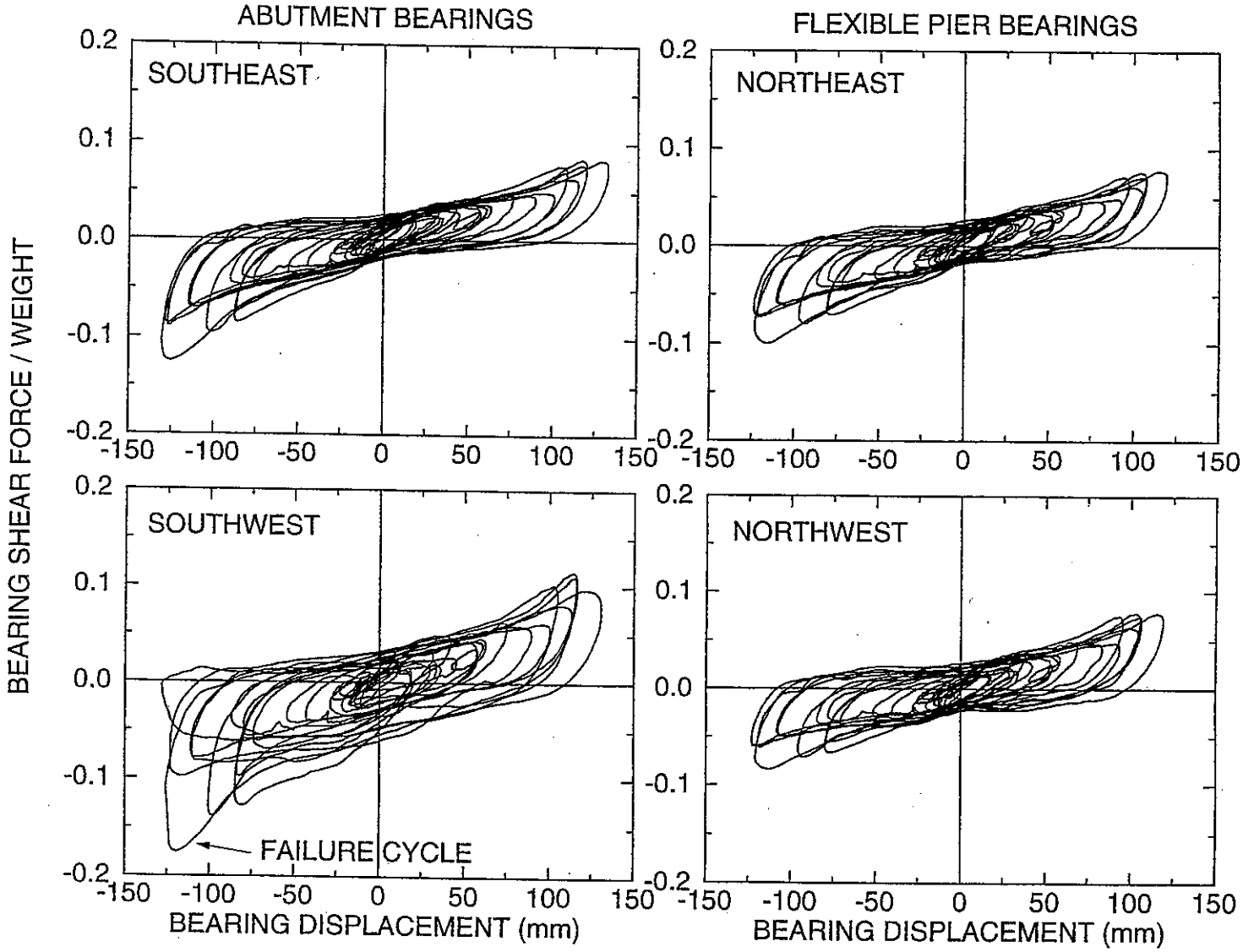

Figure 6-8: Shear Force-Displacement Loops of High Damping Elastomeric Bearings in Failure Test (Japanese Level 2, Ground Condition 3, Test No. H0FS025.001)

Figure 6-9 shows a view of the failed bearing in which the failure region is visible. Note that the bearing still carries the weight of the deck but it has some distortion as well as visible bulging of individual layers. The bulging was the result of excessive creep and it was present before the failure test (actually, both bearings from batch No. 1 had similar bulging). The failure of the bearing was not apparent during testing. Rather it was detected afterwards due to the permanent distortion of the bearing. It should be recognized that this failure was dependent on the condition of the bearings (improperly cured) and the nearly unstable condition of their operation. It is impossible to extrapolate the failure results to the scale of prototype bearings. Nevertheless, it is encouraging to observe that the failure was not catastrophic.

6.3.4 Comparison of High Damping Elastomeric System and Linear Viscous Damper System

Comparison of the two systems is interesting because they primarily differed in their damping characteristics with the system with linear dampers having approximately twice the effective damping of the high damping elastomeric system. However, the comparison is limited by the fact of not having tested the high damping elastomeric system with the records from the 1994 Northridge and 1995 Kobe earthquakes.

Nevertheless, a good picture of the behavior of the two systems is provided in Figure 6-10 where the peak response of the two systems is presented as a function of the peak table velocity. It is evident that the system with linear viscous dampers has substantially less bearing displacement and flexible pier shear force response than the high damping elastomeric system. Moreover, the two systems have about the same total shear force at the isolation level. However, due to the redistribution of this force provided by the viscous dampers, more force is transmitted to the strong abutment by the system with dampers.

Interesting observations can be made when the response of the two systems is directly compared for the same or nearly the same seismic input. For this comparison we choose the El Centro S00E and the Pacoima Dam S16E inputs. Figures 6-11 and 6-12 present comparisons of the recorded time histories of abutment bearing displacement, loops of isolation system force versus abutment bearing displacement and loops of flexible pier shear force versus pier drift of the two systems.

For the case of El Centro S00E 200% (Figure 6-11), the input in the two tests was essentially the same. The benefits offered by the viscous damper system are apparent and significant: reduction of bearing displacement to about half without any increase in the isolation system total shear force.

For the case of Pacoima Dam S16E (Figure 6-12), the input in the two tests is not the same. The input in the case of the system with dampers is stronger with the peak table velocity being nearly 40-percent larger than that of the input in the case of the high damping elastomeric system. Despite the difference in the intensity of the input, the system with viscous dampers undergoes substantially lesser displacement response (approximately half) while the peak isolation system force is nearly the same in the two systems.

Figure 6-9: View of Failed Bearing (note that it still carries the weight of the deck)

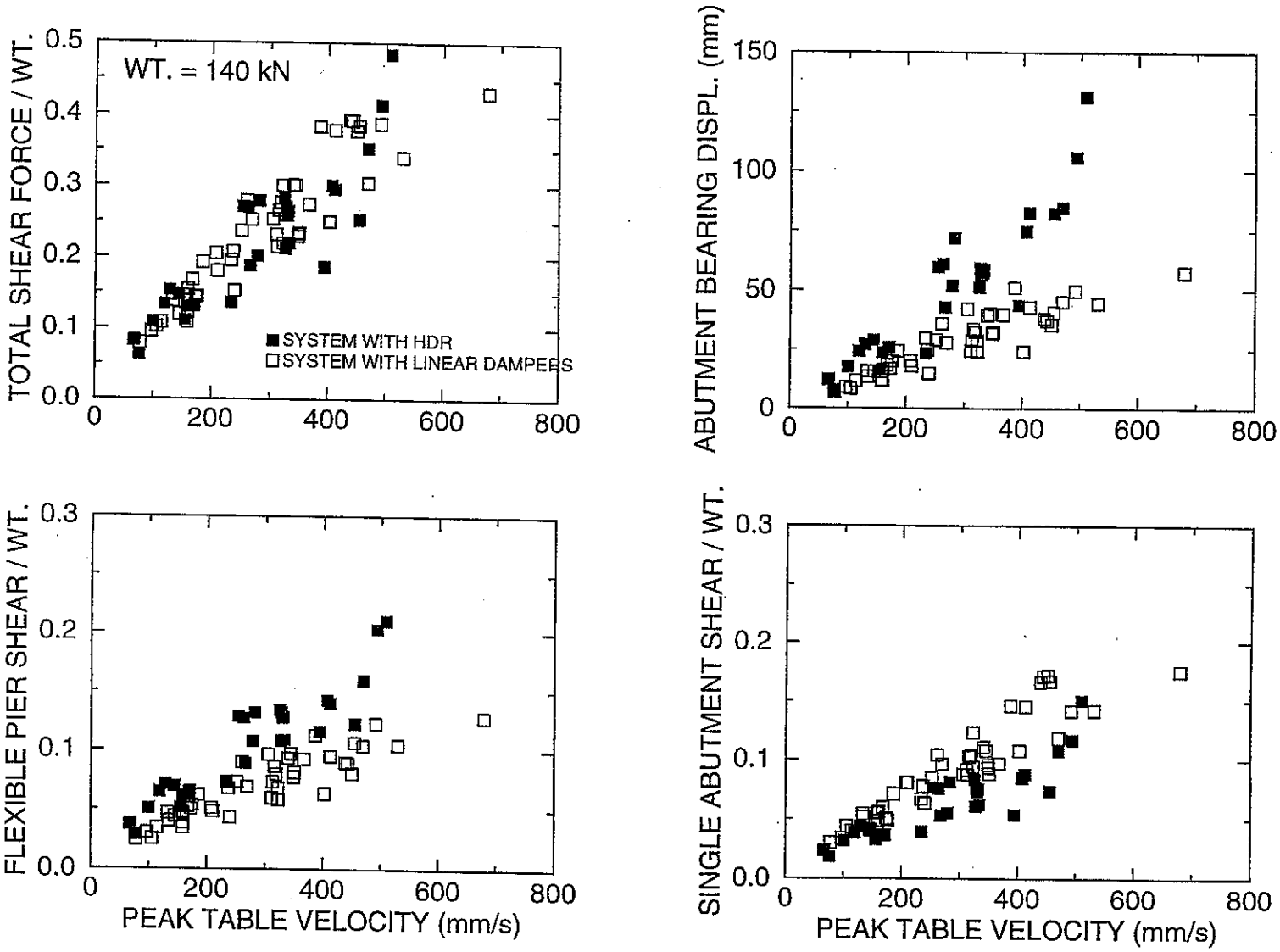

Figure 6-10: Comparison of Peak Response of Isolated Bridge with High Damping Elastomeric System and with Linear Viscous Damper System

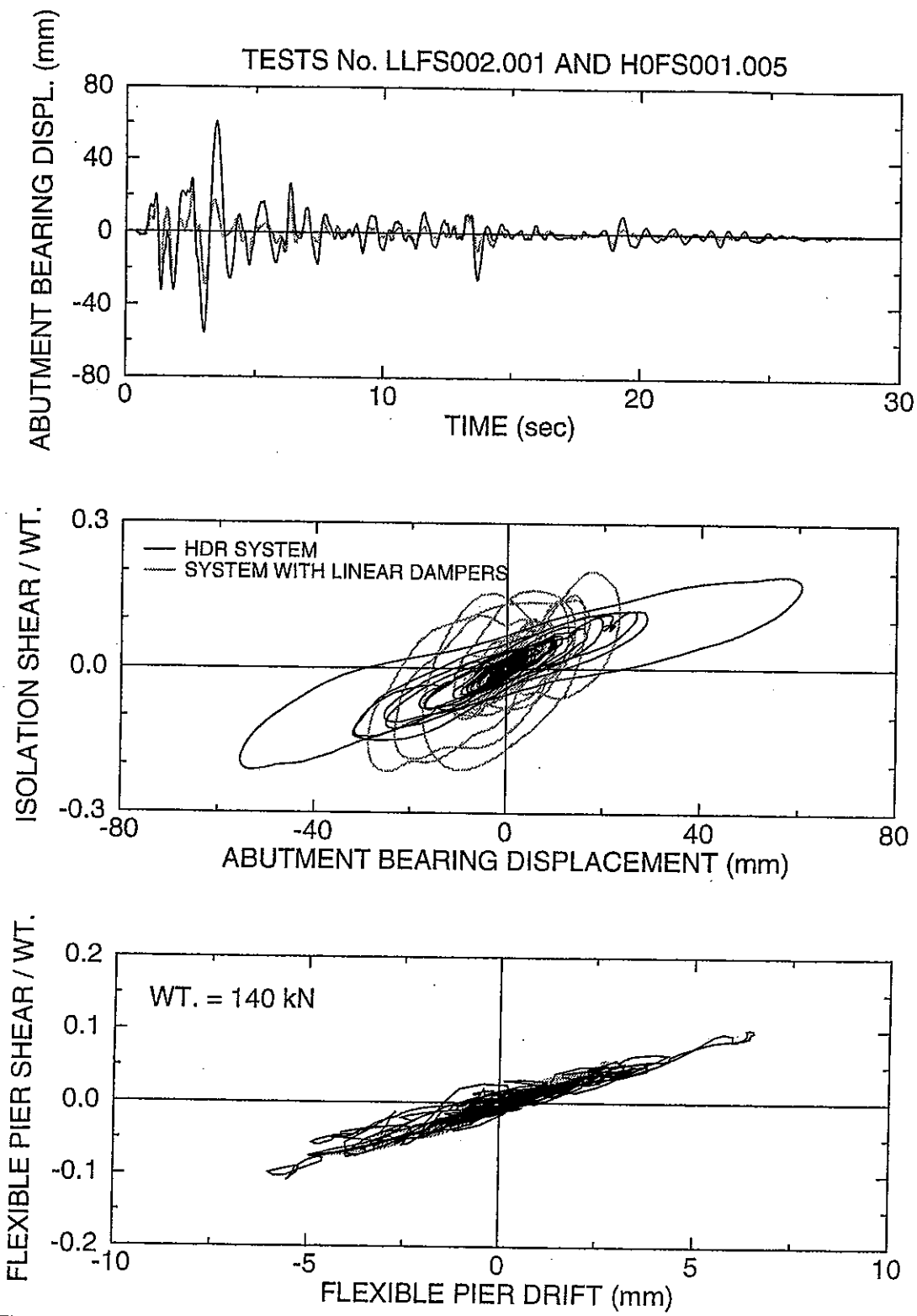

Figure 6-11: Comparison of Response of Isolated Bridge with High Damping Elastomeric System and with Linear Viscous Damper System for the El Centro S00E 200% Input

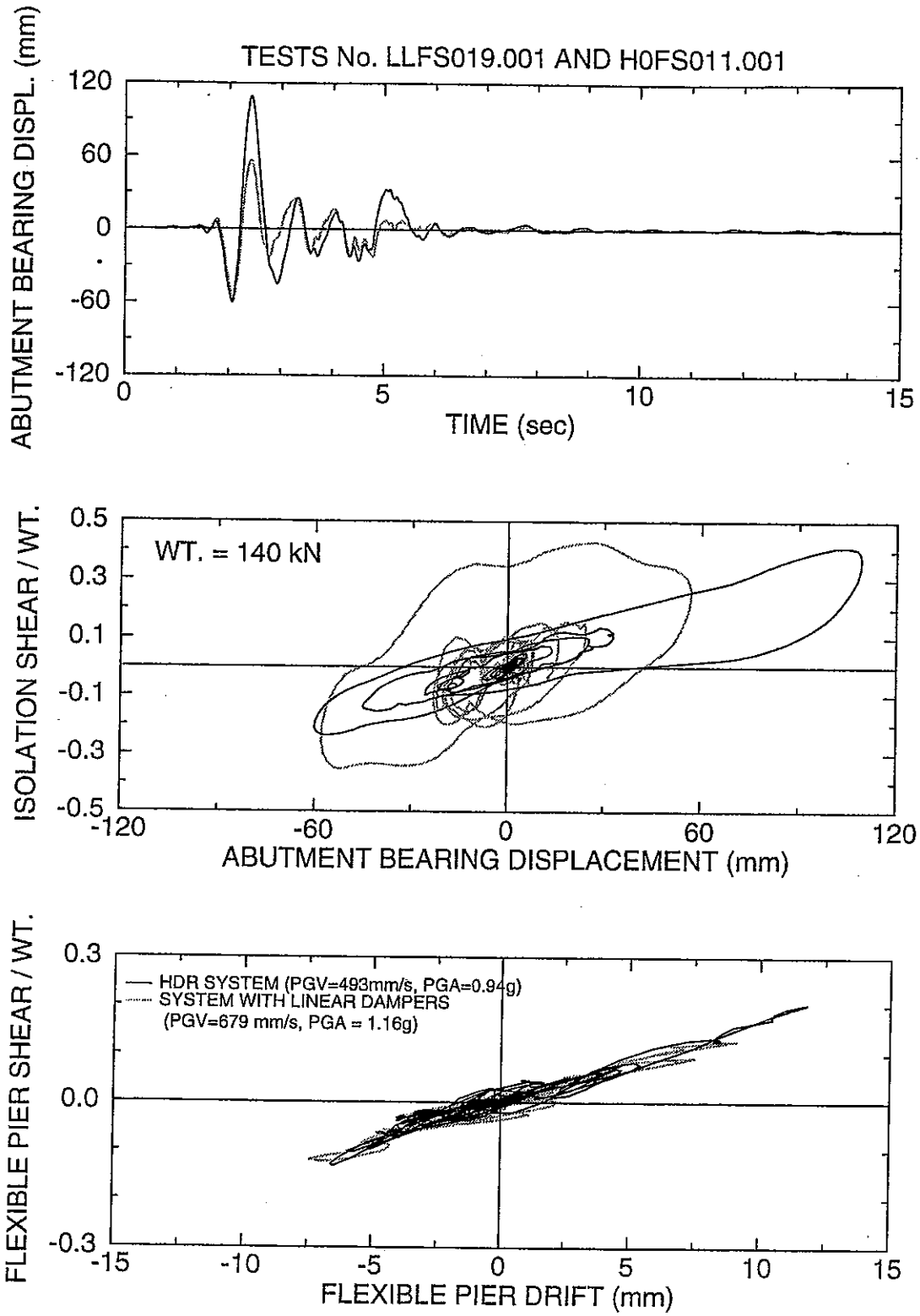

Figure 6-12: Comparison of Response of Isolated Bridge with High Damping Elastomeric System and with Linear Viscous Damper System for the Pacoima Dam S16E Input

Concluding, we note that the use of viscous damping in the isolation systems is particularly beneficial in reducing the displacement response. However, it should also be noted that for the tested systems, the resulting substructure forces for strong seismic excitation were large and of about the same magnitude whether the dampers were utilized or not. Reduction of these forces may be accomplished by the use of more flexible elastomeric bearings together with viscous dampers.

6.3.5 Comparison of Isolated Systems with Linear and Nonlinear Viscous Dampers

The nonlinear viscous dampers were designed to deliver the same force as the linear dampers at the velocity of 350 mm/s along the axis of the damper. For the angle of 45 degrees of placement of the dampers, this limit on velocity corresponds to approximately 495 mm/s relative velocity at the isolation system level in the longitudinal bridge direction. Such high relative velocities were not reached in the majority of tests of the isolated bridge with dampers. Accordingly, in most tests the nonlinear viscous dampers mobilized a substantially larger damping force than the linear dampers. The result was a further reduction in the bearing displacement at the expense of increased total shear force at the isolation system. Figure 6-13 presents a comparison of recorded isolation system loops of the two systems in identical or nearly so seismic excitations. These tests were selected to demonstrate the substantial effect of the nonlinear dampers to further reduce displacement and without or with minor increase in the peak isolation system force.

A different picture emerges in the comparison of loops obtained in motions characterized by near-fault conditions, which are presented in Figure 6-14. It is observed that in all three cases of input the bearing displacements are nearly the same for the systems with linear and with nonlinear dampers. We investigate this further by differentiating the records of damper displacements to obtain the peak damper velocities. They are presented in Table 6-2 together with measured values of the peak damper forces. Clearly, the achieved velocities exceed the limit of 350 mm/s for which the two dampers were designed to deliver the same damping force. The effect is that the nonlinear dampers mobilized lesser peak damping force than the linear ones as it is also evident in the loops of Figure 6-14. This provides an explanation for the observed behavior.

Table 6-2: Peak Damper Velocities and Forces in Tests with Motions Having Near-Fault Characteristics

INPUT MOTION	LINEAR DAMPERS				NONLINEAR DAMPERS			
	TEST No.	PEAK TABLE VEL (mm/s)	PEAK DAMPER VEL[1] (mm/s)	PEAK DAMPER FORCE[1] (kN)	TEST No.	PEAK TABLE VEL (mm/s)	PEAK DAMPER VEL[1] (mm/s)	PEAK DAMPER FORCE[1] (kN)
NORTHRIDGE NEWHALL360°	LLFS036.1	438	359	28.1	LNFS037.1	451	419	25.0
KOBE NS	LLFS039.1	450	386	31.3	LNFS039.1	448	461	25.8
PACOIMA DAM S16E	LLFS019.1	679	443	35.8	LNFS022.1	492	477	26.2

1: Each Damper (values in two dampers were slightly different; reported value is average)

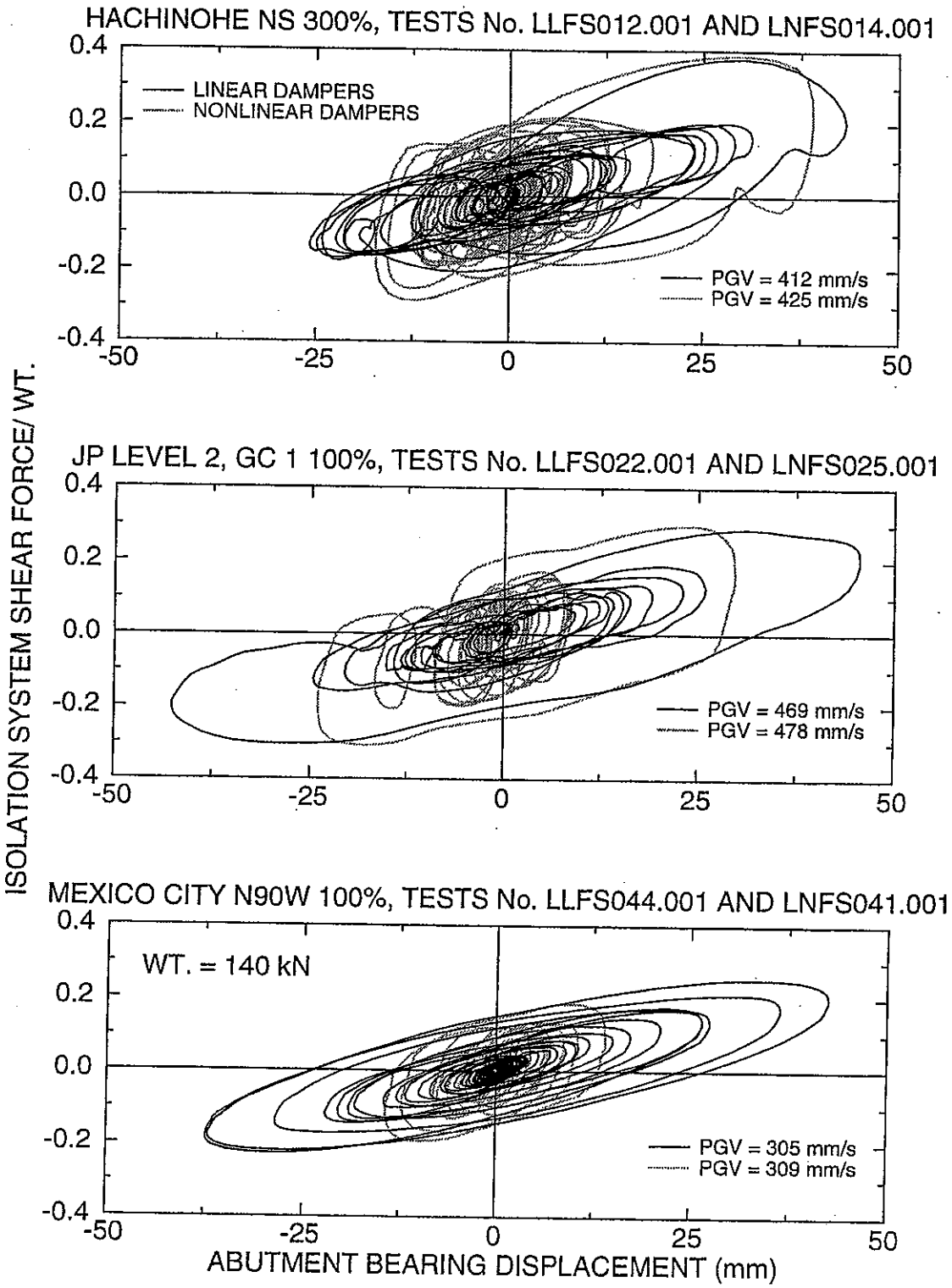

Figure 6-13: Comparison of Isolation System Force-Displacement Loops of Systems with Viscous Dampers in Selected Motions

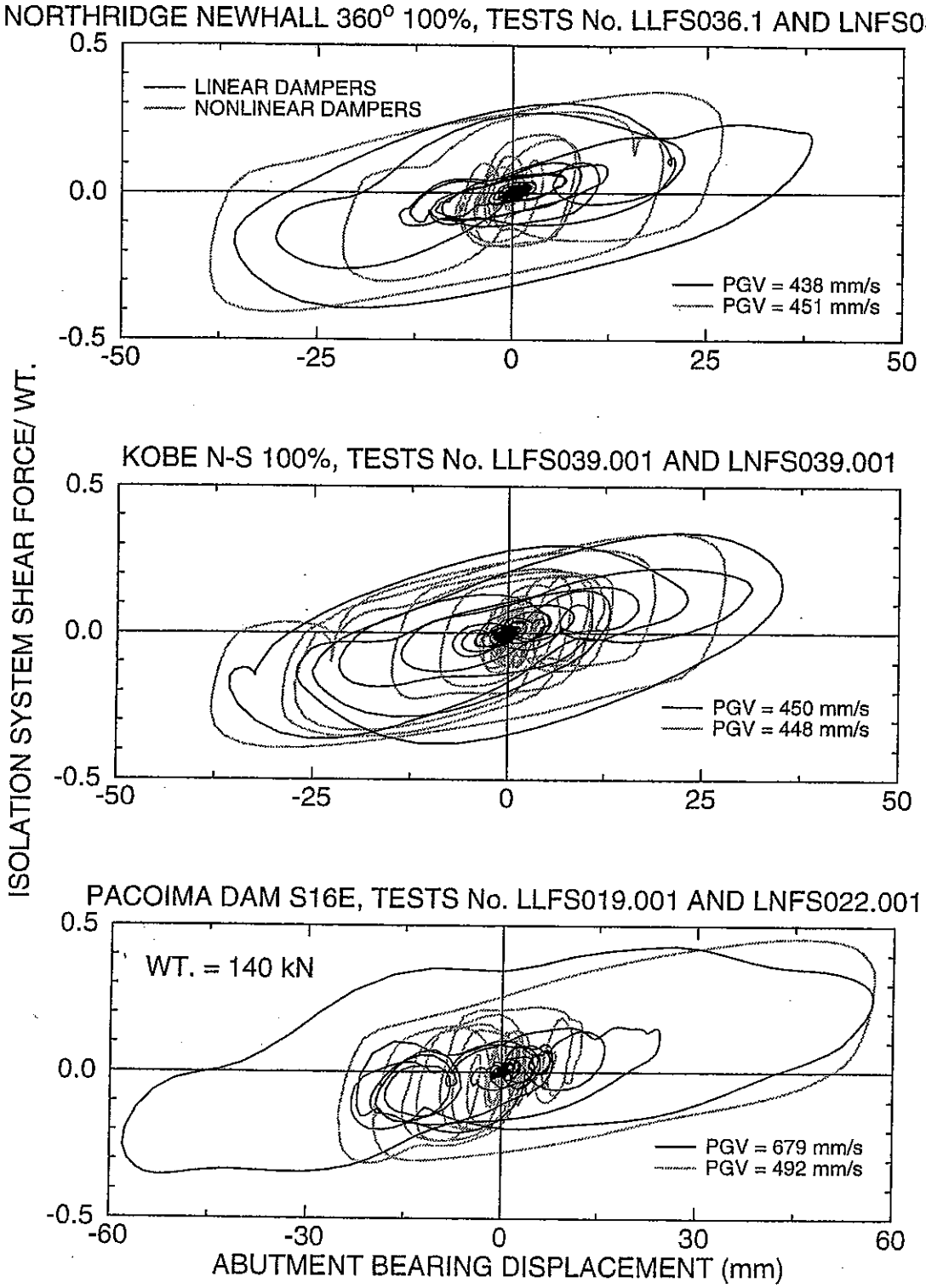

Figure 6-14: Comparison of Isolation System Force-Displacement Loops of Systems with Viscous Dampers in Selected Motions with Near-Fault Characteristics

An interesting observation may be made in the results of Figure 6-14. The system with the nonlinear dampers has a slightly larger peak isolation system force than the one with linear dampers, whereas both undergo about the same peak displacement. One may question the benefit offered by the nonlinear dampers. To discuss this we start with an explanation for this behavior. Simply, the nonlinear dampers mobilize a larger damping force at low velocities, that is, at displacements near their peak value. The result is obvious when considering that the isolation system force is the superposition of the damping and the restoring (from the bearings) forces.

The benefit, then, offered by the nonlinear dampers is to achieve a behavior comparable to that of the linear dampers with a lesser peak damping force (provided that velocities are large enough). The result is lower cost for the damper and connections, and lesser uncertainty in the value of peak damper force. It becomes now obvious that an optimal design of the nonlinear dampers is to have linear behavior for a range of low velocities (which, however, depends on the characteristics of the input motion) and nonlinear behavior for large velocities.

It is interesting to study the time histories of the bearing displacements for the two systems in the motions with near-fault characteristics, as shown in Figure 6-15. The following are observed:

(a) The peak response occurs as the result of some strong velocity shock in the input, which is preceded by input of lesser intensity.

(b) During excitation by the preceding input, the system with nonlinear dampers undergoes lesser displacement than the system with linear dampers due to the substantially larger damping force that the nonlinear dampers deliver.

(c) At the instant of application of the strong velocity shock, the two systems are at different stages of motion in terms of both displacement and velocity with respect to the table. That is, while the two systems are subjected to same, more or less, velocity shock, they undergo motion thereafter that depends on their characteristics (in this case they differ by the damping force they deliver) and their initial conditions (which are different due to the effects of the preceding seismic input). It just happens that they end up with the same peak displacement.

(d) In the motion that follows the peak response (primarily free vibration response), the system with nonlinear dampers undergoes progressively lesser displacement response due to its higher damping.

It should be clear now that the conditions of movement (the initial conditions) at the instant of application of the strong velocity shock have a significant impact on the peak response of the system. To elucidate this we present analysis results of a simple system subjected to ground shock. We consider a rigid mass supported by an isolation system which has linear elastic and viscous characteristics with period equal to 1.0 sec and damping equal to 0.30 (that is, very similar to the tested system with linear viscous dampers). It is subjected at the ground with half cycle of sinusoidal acceleration history of peak velocity equal to 0.5 m/s and duration equal to 0.2 sec. The relative displacement is numerically calculated on the assumption of zero initial conditions and then again with nonzero initial velocity conditions. The time histories of displacement are presented in Figure 6-16. The results clearly demonstrate the importance of initial conditions. It may be recognized that for this case of a linear-viscous system the total response is simply the superposition of the response due to the input for zero initial conditions and the free vibration response due to the initial conditions.

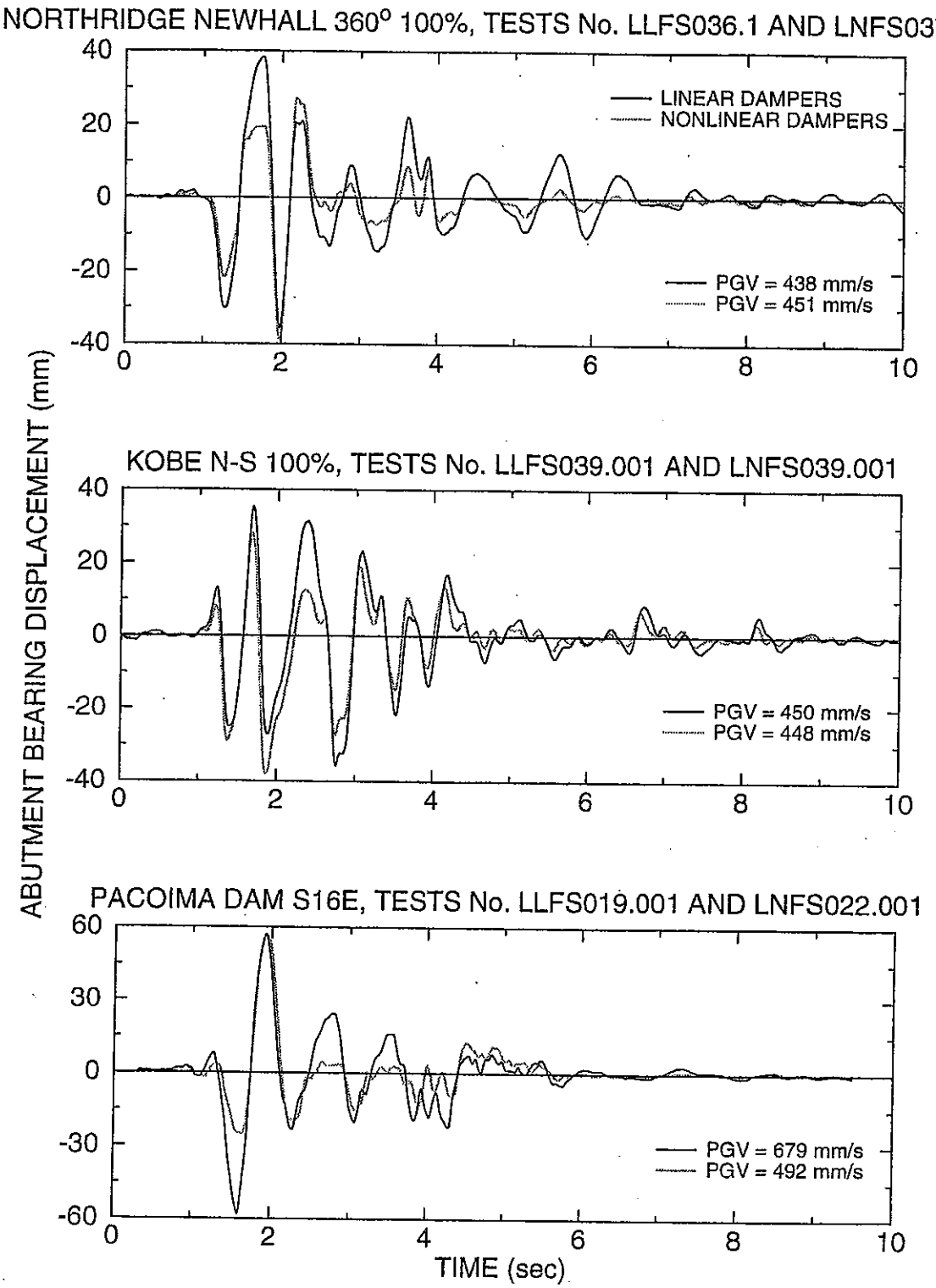

Figure 6-15: Comparison of Time Histories of Abutment Bearing Displacement of Systems with Viscous Dampers in Selected Motions with Near-Fault Characteristics

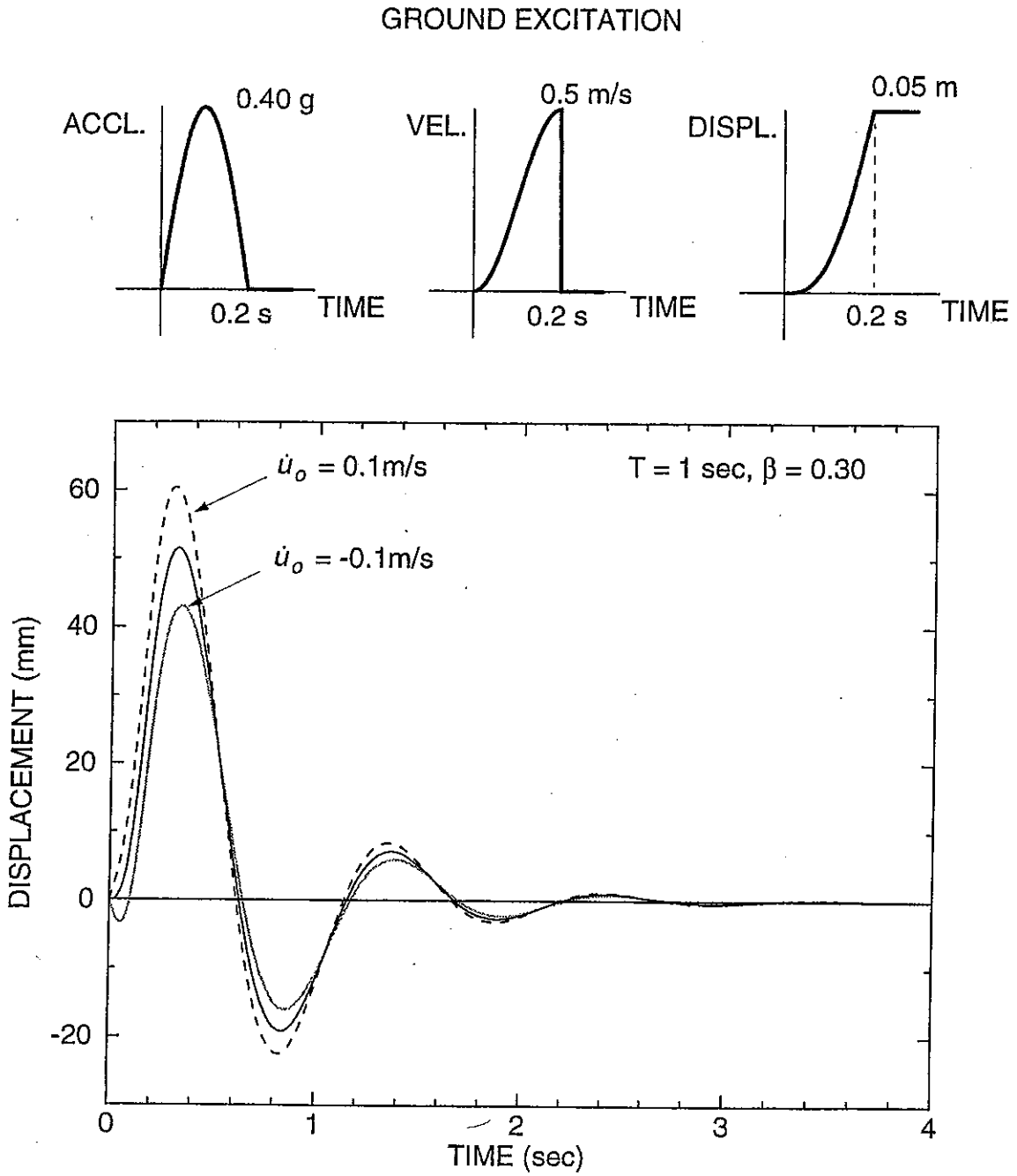

Figure 6-16: Calculated Displacement Histories of Linear-Elastic, Viscous Oscillator Subjected to 0.5 m/s Velocity Shock and Having Zero and Non-zero Initial Conditions of Velocity

6.3.6 Effect of Vertical Ground Acceleration

A number of tests were conducted with horizontal only excitation and then again with combined horizontal and vertical excitation. The results in Table 6-1 demonstrate minor effect on the isolation system force and displacement but some effect on the flexible pier shear force and drift. The effects seen on the drifts of the pier and abutment may be entirely the result of vertical vibration in the instruments used to measure displacement. The same phenomenon occurs in the instruments used to measure the bearing displacements but the effect is insignificant due to the much larger displacements of the bearings by comparison to the pier and abutment drifts. Moreover, the recordings of pier shear forces may have been also affected by the vertical excitation. Note that the strain gauge shear load cells in the columns of the flexible pier were calibrated in the absence of vertical load. Accordingly, the measurement may be affected by the vertical load, particularly when is variable.

Figures 6-17 and 6-18 present comparisons of the recorded response of two of the tested isolation systems in tests without and with the vertical ground component. The effects of vertical ground acceleration are clearly insignificant.

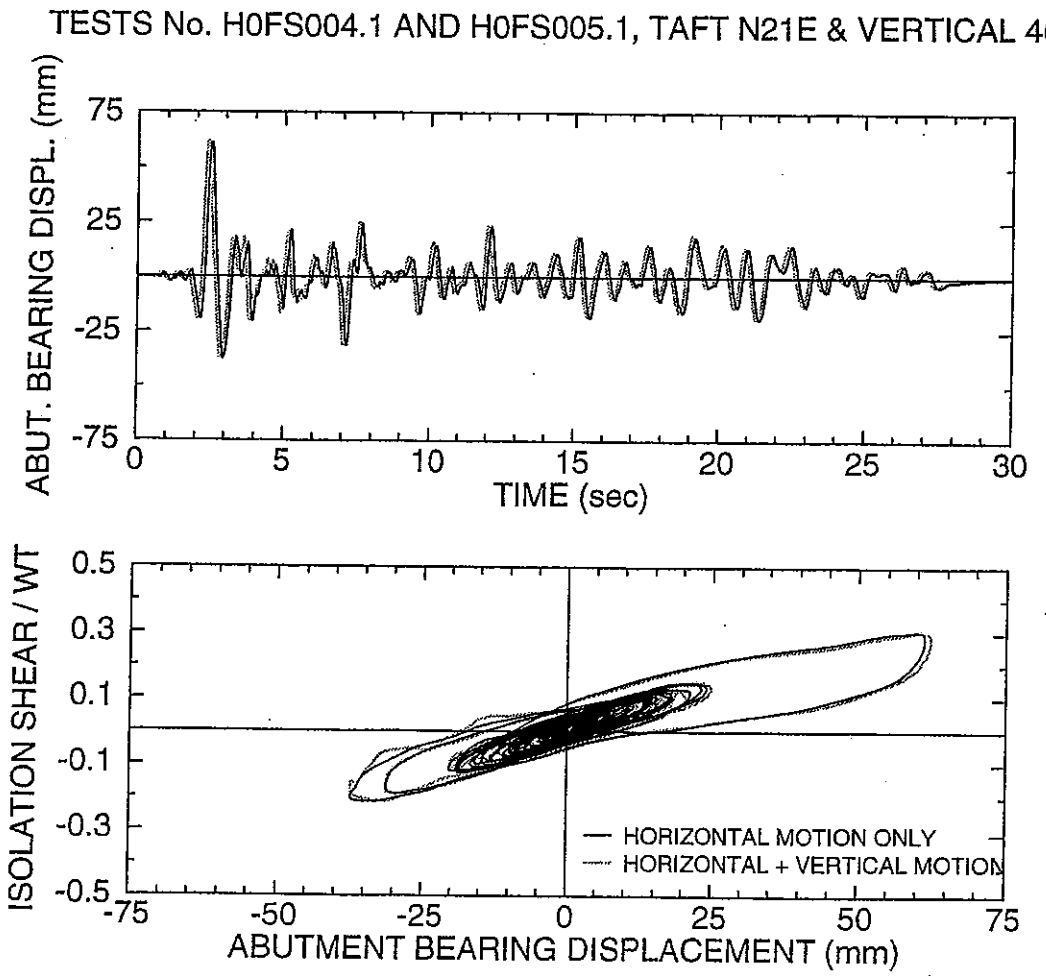

Figure 6-17: Effects of Vertical Acceleration on the Response of High Damping Elastomeric Isolation System

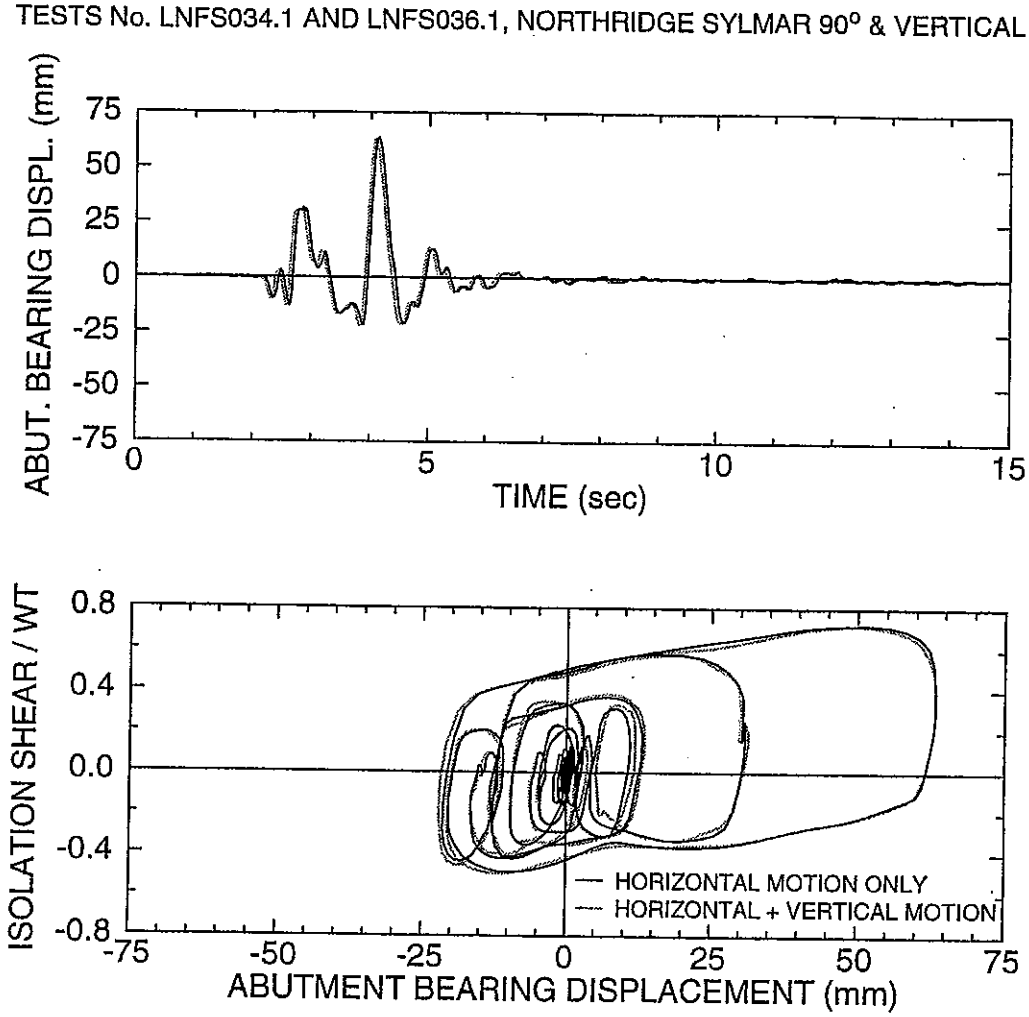

Figure 6-18: Effect of Vertical Acceleration on the Response of Elastomeric Isolation System with Nonlinear Dampers

It is of interest to note that significant vertical accelerations were recorded in the vertical direction at the bases of the abutment and flexible pier during these tests. For example, in the testing of the high damping elastomeric system with the Taft N21E and Vertical at 400% (test No. H0FS005.1) the vertical accelerations reached 0.69g. Figure 6-19 shows the recorded axial load on the abutment southeast bearing as function of the bearing horizontal displacement in this test and in the test without the vertical component of excitation (test No. H0FS004.1). The figures show the records for a time window corresponding to the maximum bearing exertion. It may be observed that there is a significant variation in the axial load which is consistent with the recorded peak vertical acceleration. The axial load varies between about 8 and 60 kN, whereas the gravity load for this bearing was 36.3 kN. Despite this significant variation we observe an insignificant effect on the response of the isolated bridge, which is primarily manifested as waviness in the loops as seen in Figure 6-17. It is also interesting to observe that the peak axial load on the bearing occurs at a substantial lateral displacement, which in this case is about 2/3 of the peak displacement.

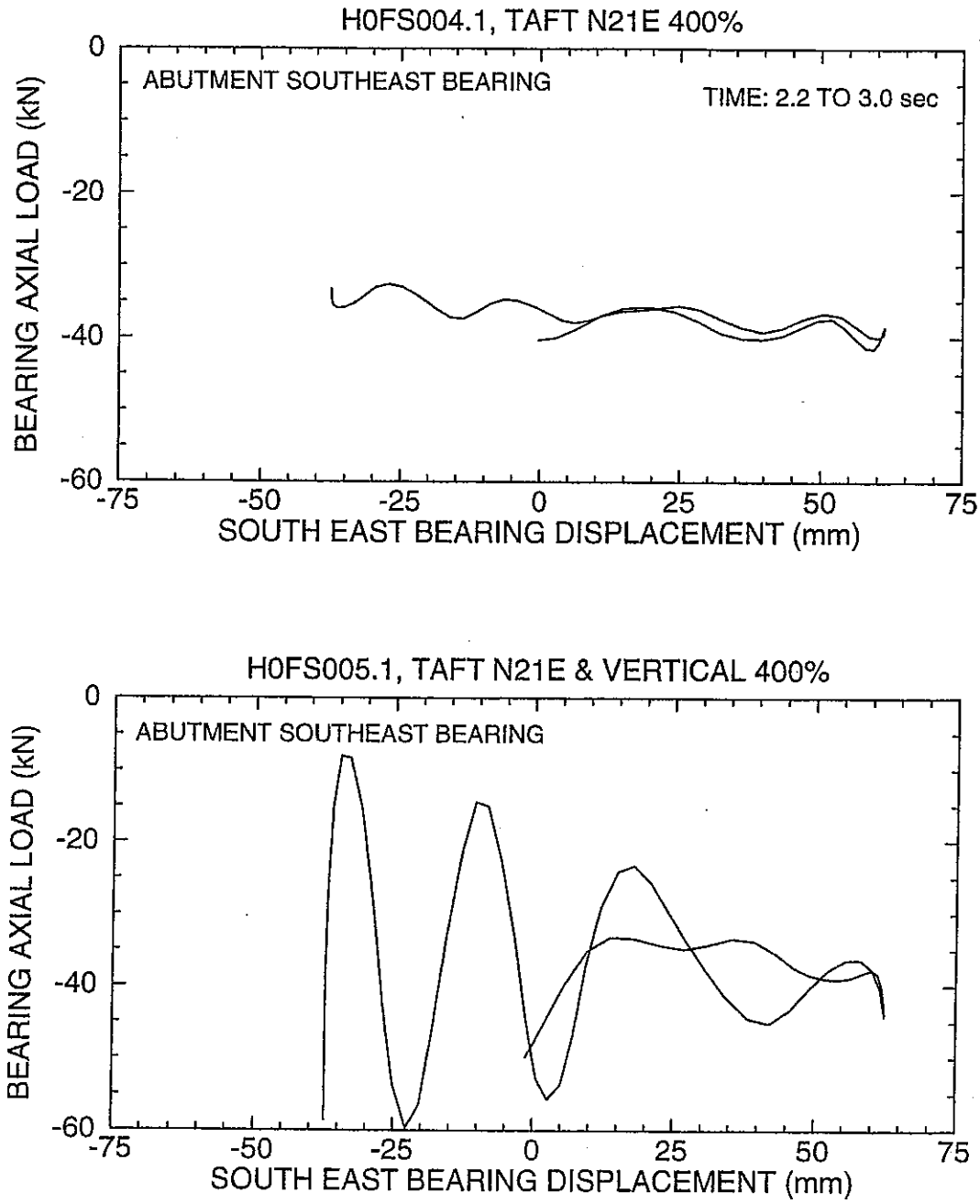

Figure 6-19: Recorded Axial Load on Bearing as Function of Lateral Displacement in Testing of the High Damping Elastomeric Isolation System

6.4 Conclusions

The testing of the elastomeric isolation systems allowed for a number of interesting observations. One is on the effect of the scragging phenomenon in the case of the high damping elastomeric systems. Consideration of only the scragged properties of the bearings and neglect of the likelihood of full recovery to the unscragged conditions could result in substantial underestimation of the inertia forces. In the conducted tests this underestimation was of the order of 30-percent. This results provides justification for the requirement in the 1997 AASHTO (American Association of State Highway and Transportation Officials, 1997) to consider the scragging and recovery phenomenon in the analysis of isolated bridges.

Damping in high damping elastomeric bearings is, as expected beneficial in the reduction of displacement and accordingly of inertia forces. This has been observed throughout the testing except for motions with strong near-source characteristics. In this case, the amount of damping provided by the high damping elastomeric bearings did not offer any advantage over the low damping elastomeric bearings in reducing either the displacement or the force response of the tested bridge. This phenomenon has been explained on the basis of different initial conditions in the motion of the two systems at the instant of application of the velocity shock in the near-fault seismic input. Stated differently, the additional damping provided by the high damping elastomeric system was insufficient to affect the response of the system in the seismic motions with strong near-source characteristics.

However, the addition of viscous damping, whether of linear or nonlinear nature, provided for a marked reduction in the displacement response without an increase in the isolation system force. It appears that significant added damping is needed in isolated structures at locations susceptible to seismic motions with strong near-source characteristics. The experiments provided data that in motions with strong near-source characteristics, such as the Pacoima Dam S16E input, added linear viscous damping of the order of 30-percent of critical are needed to reduce displacement to low levels. While the recorded displacements were exceptionally low, they were achieved at the expense of damper forces with horizontal components of the order of 25-percent of the deck weight.

The use of properly designed nonlinear dampers produces results comparable to those of the linear dampers in motions with strong near-source characteristics, however with lower peak damper forces. As seen fro example in Table 6-2, the nonlinear dampers operated at peak forces of about 10 to 20-percent lower than the peak forces in the linear dampers while the isolated bridge response in terms of the peak displacement and peak isolation system shear force were about the same. This represents the main advantage offered by the nonlinear dampers.

Another interesting observation made in the testing of the elastomeric isolation systems is the minor effect of the vertical ground acceleration on the response of these systems. While significant fluctuations in the axial load on the bearings were recorded, they had a negligible effect on the behavior of the system.